DOI: 10.7860/JCDR/2022/53056.16482

Original Article

Radiology Section

Association between Chest CT Severity Scores and SARS-CoV-2 Vaccination among COVID-19 patients: A Cross-sectional Study from Pune, India

ASHISH LAXMAN ATRE[1], AKHIL ATRE[2], SUHRUD PANCHAWAGH[3], RAHUL KHAMKAR[4], APARNA CHANDORKAR[5], SUNIL PATIL[6]

ABSTRACT

Introduction: The novel Coronavirus disease-2019 (COVID-19) caused by Severe Acute Respiratory Syndrome Coronavirus 2 (SARS-CoV-2) is seen to primarily affect the human respiratory system. Chest CT Severity Score (CTSS) provides a semi quantitative assessment of pulmonary involvement in COVID-19 patients. COVID-19 pandemic mitigation measures such as SARS-CoV-2 vaccination are being deployed worldwide. However, with the emerging variants of concern of SARS-CoV-2, a high prevalence of post vaccination breakthrough infections is seen.

Aim: To assess the association of CTSS with the vaccination status in a cohort of COVID-19 patients referred to a tertiary diagnostic centre and to evaluate the association of CTSS with other clinical parameters including co-morbidities in these patients.

Materials and Methods: This cross-sectional observational study was conducted at a tertiary care diagnostic imaging centre in the city of Pune, Maharashtra, India. Data of 1002 symptomatic, adult patients who underwent chest CT and SARS-CoV-2 Reverse Transcription Polymerase Chain Reaction (RT-PCR)/Rapid Antigen Test (RAT) laboratory test between March 13, 2021 and June 22, 2021, were collected. COVID-19 reporting and Data System (CO-RADS) categories and the corresponding semi quantitative CTSS were calculated for each patient. Based on their vaccination status, patients were categorised into three groups: unvaccinated, partially vaccinated and fully vaccinated. The association of CTSS with various categories of vaccination status, demographics, co-morbidities and stages of the disease of the patients, was evaluated.

Results: Of the 1002 COVID-19 patients, 768 (76.6%) were unvaccinated, 190 (19.0%) were partially vaccinated and 44 (4.4%) were fully vaccinated. Mean CTSS in the fully vaccinated cohort was significantly lower (3.75±4.7) than that in the partially vaccinated (6.05±5.7) and unvaccinated (8.29±4.9) patients (mean 3.75 vs. 6.05 vs. 8.29, respectively; ($p<0.05$). Mean CTSS in patients with no co-morbidities was significantly lower than that in patients with hypertension and diabetes (7.12 vs. 8.75 vs. 10.39, respectively; ($p<0.05$).

Conclusion: Significant association was noted between the Chest CTSS and the vaccination status, age, gender, co-morbidities and stage of disease in this large cohort of COVID-19 patients. The study reiterates that full vaccination aids in reducing the severity of lung involvement in COVID-19 infection.

Keywords: Computed tomography, Coronavirus, Diagnostic imaging, Immunisation, Respiratory tract infections

INTRODUCTION

High Resolution Computed Tomography (HRCT) of the chest plays a pivotal role in assessing the severity of lung involvement in novel Coronavirus disease-2019 (COVID-19) infection [1-3]. The COVID-19 Reporting and Data System (CO-RADS) and the corresponding CT Severity Score (CTSS) introduced by Radiological Society of the Netherlands provide a semi quantitative assessment of virus induced pulmonary involvement [4,5].

Mass vaccination is considered to be an important tool for COVID-19 disease prevention. India's COVID-19 vaccination program was expanded to include all citizens ≥18 years of age, even as the country witnessed a massive surge in infections during the 2nd wave of the pandemic [6]. The ChAdOx1n CoV-19/Covishield and BBV152/Covaxin are the two vaccines approved for emergency use in India [7]. However, vaccines do not confer complete immunity against the viral disease and vaccine breakthrough infections are being reported [8,9].

Studies have reported that chest CTSS correlates with the extent of lung damage in COVID-19 patients and therefore, may be used as a novel indirect indicator of vaccine effectiveness in the real world settings [2,3,10]. Studies comparing the chest CTSS and vaccination status among Indian patients with COVID-19 infection are scarce (one of these studies was a preprint at the time of writing this paper) [11-13].

On this background, the present study aimed to assess the association between chest CTSS and vaccination status in a cohort of Indian patients with COVID-19 infection. The secondary objective of this study was to assess the correlation between CTSS and the clinical parameters including co-morbidities in these patients.

MATERIALS AND METHODS

This cross-sectional, observational study was conducted at the imaging clinics of a tertiary diagnostic centre, in Pune, Maharashtra, India, between March 13, 2021 and June 22, 2021. This tertiary care diagnostic imaging centre receives referrals from various parts of Pune district. The study was approved by Institutional Ethics Committee (ECR/311/INST/MH/2013/RR-19) and informed consent was obtained from all the patients.

Sample size calculation: Optimum sample size for the study was estimated using the formula: $N=(1.96)^2 PQ/L^2$. Where, N=Sample size, 1.96= Standard normal deviate set corresponding to 95% confidence interval (CI), P=Percentage of vaccinated population in

Pune district till June 2021, Q=100-P and L=Permissible error in estimation i.e., 10% of P.

Percentage of vaccinated population in Pune district till June 2021 (P), was calculated using the formula: P=total number of SARS-CoV-2 vaccinations done in Pune district till June 2021 i.e., 32, 17, 978 persons×100/total population of Pune district i.e.,1, 00, 89, 916 persons, estimated in accordance with the Aadhaar uidai.gov.in December 2020 data [14-16]. Thus, the sample size calculated for this study was 820 patients [Table/Fig-1]. Taking into consideration the possible loss to follow-up of 20 % in an urban setting, the estimated optimum sample size for this study was further increased to 984 patients [Table/Fig-1]. The present study therefore included 1002 patients with COVID-19 infection.

P (%)	Q=100-P	L=10% of P	$N=(1.96)^2 PQ/L^2$	Loss to follow-up =20% of N	Optimum sample size=N+ Loss to follow-up
31.9	68.1	3.19	$820=(1.96)^2 \times 31.9 \times 68.1/(3.19)^2$	164	984 =820+164

[Table/Fig-1]: Optimum sample size calculation using the formula: $N=(1.96)^2 PQ / L^2$
P: Percentage of vaccinated population in Pune district till June 2021; Q: 100-P; L: Permissible error in estimation i.e., 10% of P; N: Sample size; 1.96: Standard normal deviate set corresponding to 95% confidence interval.

Inclusion criteria:

- Age ≥18 years;
- Patients suspected to have symptoms of COVID-19 infection;
- Patients who were referred for HRCT chest between March 2021 and June 2021;
- Patients with a positive SARS-CoV-2 Reverse Transcription Polymerase Chain Reaction (RT-PCR)/Rapid Antigen Test (RAT).

Exclusion criteria: Pregnant women, patients <18 years of age and patients with a negative RT-PCR/RAT test.

Study Procedure

Data collection: Clinical data, laboratory data (SARS-CoV-2 RT-PCR/RAT tests) and vaccination data of the study patients were collected from electronic medical records, patient's clinical history sheets, and from telephonic interviews. Clinical information collected from all study patients included: age, gender, co-morbidities and stage of illness based on the time interval between onset of symptoms and acquisition of chest HRCT scan.

Chest HRCT evaluation: As a standard of practice, non contrast chest HRCT scans of the COVID-19 patients were performed on a multidetector CT scanner (Philips Ingenuity 128 Slice CT; Philips Healthcare, Amsterdam, Netherlands and GE 32 Slice; GE Healthcare, Waukesha, USA) with the patient in supine position, during end inspiration. Scanning parameters were in line with the manufacturer's standard recommendations for a routine thorax scan. All CT images were reconstructed to thin slices using the Multiplanar Reformatting (MPR) technique. Appropriate infection prevention and control measures were arranged for the CT technologists and the patients.

HRCT images of the COVID-19 patients were independently examined on standardised workstations, by two radiologists with 15 years' experience in reporting chest CT images. These radiologists were blinded to the vaccination as well as co-morbidity status of the study patients. Chest CT scores for the first 30 study patients were recorded by the two radiologists independently. Intra Class Correlation (ICC), which is a useful statistic for estimating Inter-Rater Reliability (IRR), was calculated for these reads. The ICC for the initial 30 chest HRCT reading was found to be 0.997 with average measures (p-value=0.0001) and the estimated IRR was 99.7% [Table/Fig-2]. Hence,the chest HRCT scans of the remaining study patients, were randomly assigned to the two experienced radiologists for independent interpretation and scoring of the HRCT images.

Variables	Intra Class Correlation (ICC)[a]	95% Confidence interval		p-value
		Lower bound	Upper bound	
Single measure	0.995[b]	0.990	0.998	0.0001
Average measure	0.997[c]	0.995	0.999	0.0001

[Table/Fig-2]: Calculation of Intraclass correlation coefficient (ICC) for the first 30 study patients.
Two way mixed effects model where people effects are random and measures effects are fixed.
a. Type C intraclass correlation coefficients using a consistency definition the between measure variance is excluded from the denominator variance.
b. The estimator is the same, whether the interaction effect is present or not.
c. This estimate is computed assuming that the interaction effect is absent, as it is not estimable otherwise.

Chest CT images of these patients were evaluated using the standard, international nomenclature based on COVID-19 Reporting and Data System (CO-RADS) [Table/Fig-3a] [4]. Further, in patients with characteristic findings of COVID-19 lung involvement, a semi quantitative CT severity scoring was performed; using the scoring system which depends on the visual assessment of the extent of anatomic involvement (on a scale from 0-5) of each of the 5 lobes of the lungs [Table/Fig-3b] [17]. The total CTSS is the sum of the individual lobar scores and it ranges from 0=no involvement to 25 maximum involvement [17]. Based on the total CTSS, the severity of lung involvement in the patients was further graded into mild (CTSS of 0-8), moderate (CTSS of 9-15) and severe (CTSS of 16-25) categories. Thereafter, CT scans were further categorised into five stages based on the duration of time interval between initial symptoms' onset and performance of chest HRCT [Table/Fig-3c] [18].

a) CO-RADS Categories and the Corresponding Level of Suspicion for Pulmonary Involvement in COVID-19, as assessed on chest HRCT scans [4]

CO-RADS Category	Level of Suspicion for Pulmonary Involvement in COVID-19	CT features
0	Not interpretable	Technically insufficient scan
1	Very Low	Normal/Non infectious
2	Low	Typical for infections other than COVID-19
3	Equivocal/Indeterminate	Suggesting COVID-19, but may be seen in some other diseases as well
4	High	Imaging abnormalities suspicious for COVID-19
5	Very High	Characteristically seen in COVID-19
6	Proven (SARS-CoV-2 RT-PCR positive)	-

b) Score of individual lobes of lungs on chest HRCT [17]

Individual Lobar score	Percentage of involvement of a lobe of lung
0	No involvement
1	<5%
2	5-25%
3	26-49%
4	50-75%
5	>75%

c) Stages of lung involvement on chest HRCT based on the duration of time interval between initial symptoms' onset and performance of the CT scan [18]

Stages	Number of days between initial symptoms' onset and performance of chest HRCT
Stage -1	0-4 days
Stage -2	5-9 days
Stage -3	10-14 days
Stage -4	15-21 days
Stage -5	>21 days

[Table/Fig-3 a-c]: Various classifications and scores used for categorisation of chest HRCT scans of study patients.
CO-RADS: COVID-19 Reporting and Data System; COVID-19: Coronavirus Disease 2019; HRCT: High resolution computed tomography; SARS-CoV-2: Severe acute respiratory syndrome coronavirus 2; RT-PCR: Reverse transcription polymerase chain reaction

Vaccination status: The study patients were categorised into the following three groups, based upon their vaccination status at the time of a positive laboratory confirmation of COVID-19 infection.

1) **Unvaccinated** (never received a COVID-19 vaccine dose);
2) **Partially vaccinated** (received one dose of a two dose vaccine series, or <14 days elapsed after the 2nd dose);
3) **Fully vaccinated** (received two doses of a two dose vaccine series and ≥14 days elapsed since the second dose).

STATISTICAL ANALYSIS

Statistical analysis of the data was perfomed using Epi info software. Descriptive statistics of patient's demographics and clinical results were reported as numbers (n) and percentages (%). Quantitative continuous variables were presented as mean±standard deviation. Analysis of Variance (ANOVA) test was applied to assess the significance of association between mean CTSS and various categories of vaccination status and clinical parameters of the study participants. Kruskal-Wallis test was used for confirmation of results of multiple comparisons. The differences in grades of chest CTSS between the various categories of patients based on their demographic, comorbidity and vaccination status and stage of disease; were examined using Chi-square (χ^2) test. Multivariate linear regression analysis was used to determine the association of CTSS with the vaccination status (unvaccinated or vaccinated), comorbidity status (presence or absence of comorbidity) and stages of disease on CT. For all the statistical tests; p-value <0.05 was considered statistically significant.

RESULTS

Mean age of the 1002 patients enrolled for the study was 49.0 years±15.6 years and men constituted 64.4% of the study population. Study patients were classified into three age group categories based on the prioritisation of vaccination among the Indian population as per the directives of National Expert Group on Vaccine Administration for COVID-19 (NEGVAC) [6].

Co-morbidity data was available in 949/1002 patients. Amongst these, 249 (26.2%) patients had some co-morbidities: either hypertension or Diabetes Mellitus (DM), or a combination of both DM and hypertension, which depicts the baseline demographic and clinical characteristics of the patients [Table/Fig-4].

Out of the 1002 patients, 768 (76.6%) were unvaccinated. Details of the categorisation of the study cohort depending on their CTSS, stage of lung involvement on CT and vaccination status are presented in [Table/Fig-5]. Various grades of severity of lung involvement seen on the chest HRCT images of the study patients with COVID-19 infection are illustrated in [Table/Fig-6]. Breakthrough infections

Characteristics	Number of patients, n (%)
Total number of study patients	1002 (100)
Age in years	
Mean±standard deviation* (Range)	49.0 years±15.6 (18-90)
Age group (years) classified into three groups	
18-44	416 (41.6)
45-59	299 (29.8)
≥60	287 (28.6)
Gender	
Male	645 (64.4)
Female	357 (35.6)
Co-morbid conditions (949/1002 patients)	
No co-morbidities	700 (73.8)
Diabetes Mellitus (DM)	80 (8.4)
Hypertension	99 (10.4)
DM+Hypertension (DM+HTN)	70 (7.4)

[Table/Fig-4]: Demographic and clinical characteristics of the patient cohort.
*All data are expressed as numbers (percentage) or mean±standard deviation

Categories of study patients	Number of patients, n (%)
CTSS categories (n=1002)	
Mild (CTSS of 0-8)	590 (58.9)
Moderate (CTSS of 9-15)	315 (31.4)
Severe (CTSS of 16-25)	97 (9.7)
Staging of lung involvement on CT scan * (n=1002)	
Stage 1 (0-4 days)	251 (25.0)
Stage 2 (5-9 days)	678 (67.7)
Stage 3 (10-14 days)	51 (5.1)
Stage 4 (15-21 days)	15 (1.5)
Stage 5 (>21 days)	7 (0.7)
Vaccination status (n=1002)	
Unvaccinated	768 (76.6)
Partially vaccinated †	190 (19.0)
Fully vaccinated ‡	44 (4.4)
Type of Vaccine received (n=234)	
ChAdOx1 nCoV- 19 /Covishield	207 (88.5)
BBV152/Covaxin	27 (11.5)
Doses of vaccine received (n=234)	
1st dose	178 (76.1)
2nd dose	56 (23.9)

[Table/Fig-5]: Details of patient categorisation based on their chest CTSS, CT stage of disease and vaccination status.
*Staging of lung involvement on CT scan based on time interval between initial symptom's onset and CT scan acquisition. † Received 1st dose of a two dose vaccine series, or <14 days elapsed after the 2nd dose;
‡ Received two doses of a two dose vaccine series and ≥14 days elapsed since the second dose; CTSS: CT severity score

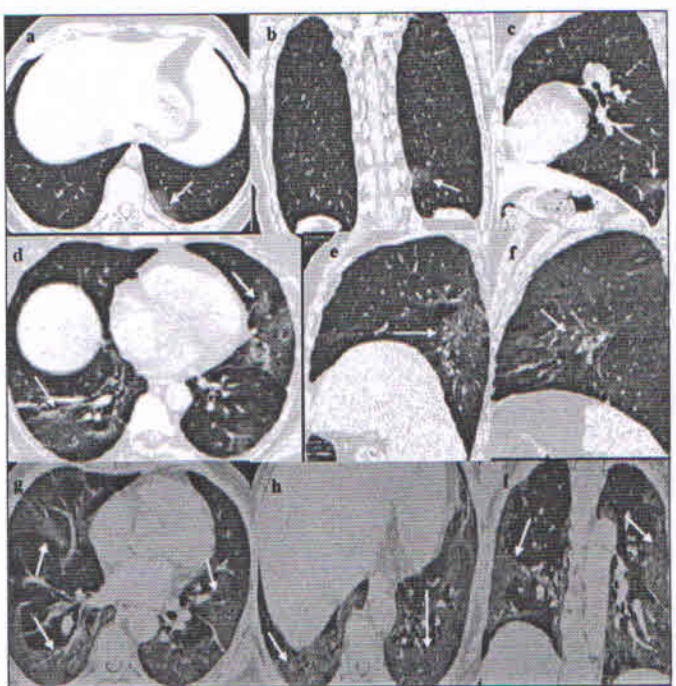

[Table/Fig-6]: Chest HRCT imaging features in study patients with COVID-19 infection: Axial (a), coronal (b) and sagittal (c) thin sections of unenhanced HRCT chest demonstrate mild sub pleural ground glass opacity (GGO) (indicated by white arrows), involving the left lower lobe in a patient with mild CTSS of 2. Bilateral, patchy, peripheral and peri broncho vascular, multi lobe GGOs (white arrows), seen on the axial (d) and sagittal sections of the right (e) and left lung (f) in another patient with moderate CTSS of 12. Axial (g,h) and coronal (i) CT sections show bilateral, diffuse areas of crazy paving pattern and peripheral consolidations in the middle and lower lobes (white arrows) of a patient with severe CTSS of 17.

(defined as SARS-CoV-2 infections occurring ≥14 days after completing the second dose of a two dose COVID-19 vaccination series); occurred in 44 (4.4%) patients.

Association of CTSS with age groups and gender: The study results showed significant difference in the mean CTSS when all the age group categories in the study population were compared together (p<0.01). Mean CTSS of the persons ≥60 years of age was

a) Age group of patients in years	Mean CTSS±SD	Number of patients (N)
18-44	6.00±5.177	416
45-59	8.35±5.511	299
≥ 60	9.34±5.801	287
Total	7.66±5.645	1002
p=0.0001 (p<0.01) by ANOVA test and Kruskal-Wallis Test (applied to confirm the results by ANOVA)		

b) Grades of CTSS based on severity of lung involvement	Number (n) and percentage (%) of patients in different age group categories (in years)			Total
Variables	18-44 years n (%)	45-59 years n (%)	≥ 60 years n (%)	n (%)
Mild (0-8)	300 (72.1)	165 (55.2)	125 (43.6)	590 (58.9)
Moderate (9-15)	96 (23.1)	97 (32.4)	122 (42.5)	315 (31.4)
Severe (16-25)	20 (4.8)	37 (12.4)	40 (13.9)	97 (9.7)
Total	416 (100.0)	299 (100.0)	287 (100.0)	1002 (100.0)
p=0.0001 (p<0.01) by Chi-square test				

[Table/Fig-7]: Comparison of Mean CTSS (a) and grades of CTSS (b) amongst different age group categories of patients.

higher than that of persons in the 45-59 years age group and 18-44 years age group (Mean CTSS 9.34 vs. 8.35 vs. 6.00, respectively) [Table/Fig-7a]. Similarly, significant difference was observed in the grades of chest CTSS of patients depending upon their age group categories. As depicted in [Table/Fig-7b], moderate as well as severe grades of CTSS were increasingly seen in the 45-59 years and ≥60 years age group categories.

The mean CTSS in male patients was significantly higher than that in the female patients (Mean CTSS 8.0 vs. 7.05 respectively) (p=0.01, p<0.05). Mild grade of CTSS was seen in greater percentage of female patients (64.1%); as compared to male patients (56%). Significant difference was detected in the grades of CTSS when compared together, based on the gender of study participants (p=0.027, p<0.05).

Association of CTSS with co-morbidities: Mean CTSS in patients with no co-morbidity was significantly lower than that in patients with comorbidities such as hypertension alone, hypertension with diabetes mellitus and diabetes alone (7.12 vs. 8.75 vs. 9.46. vs. 10.39, respectively (p<0.05) [Table/Fig-8]. Mild CTSS was seen in majority of the patients (64.3%) with no co-morbidities; whereas, highest percentage of cases (20%) with severe CTSS were seen in patients with diabetes mellitus [Table/Fig-9]. Significant difference was seen in the mean CTSS as well as in the grades of CTSS, when all groups were compared together, based on their co-morbidity status (p<0.01).

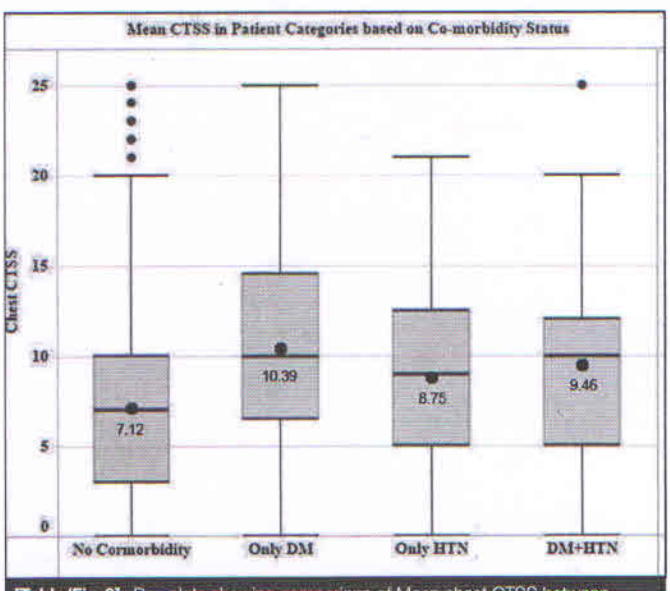

[Table/Fig-8]: Box plots showing comparison of Mean chest CTSS between patient categories based on co-morbidity status.
Blue dot within the box: Mean CTSS, Blue dots outside the box: Outliers, Black horizontal line within the box: Median CTSS.
DM: Diabetes mellitus; HTN: Hypertension; DM+HTN: Diabetes mellitus+Hypertension

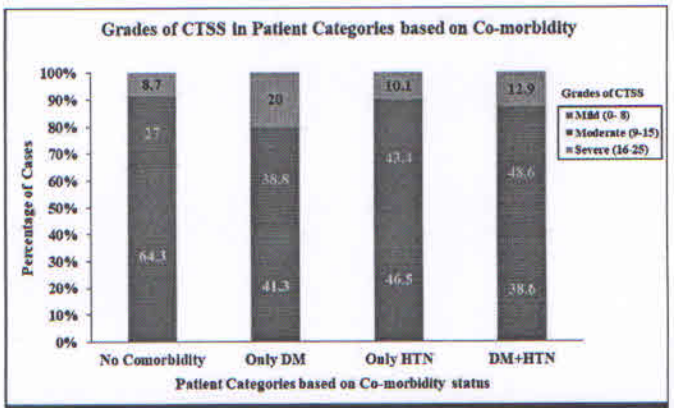

[Table/Fig-9]: Stacked column chart showing percentage distribution of grades of chest CTSS in patient categories based on co-morbidity status.
DM: Diabetes mellitus; HTN: Hypertension; DM+HTN: Diabetes mellitus+Hypertension

Association of CTSS with vaccination status: Majority of the vaccinated persons in the study cohort belonged to >60 years and 45-59 years age group. Breakthrough infections were identified in 44 (4.4%) of the vaccinated cohort. When multiple comparisons were made, mean CTSS was significantly higher in the unvaccinated cohort (mean±SD:8.29±4.9) versus the partially vaccinated patients (mean±SD:6.05±5.7) versus the fully vaccinated patients (mean±SD:3.75±4.7) (p<0.01) [Table/Fig-10]. The difference in mean CTSS between the partially vaccinated and fully vaccinated groups was also found to be significant (p=0.035, p<0.05).

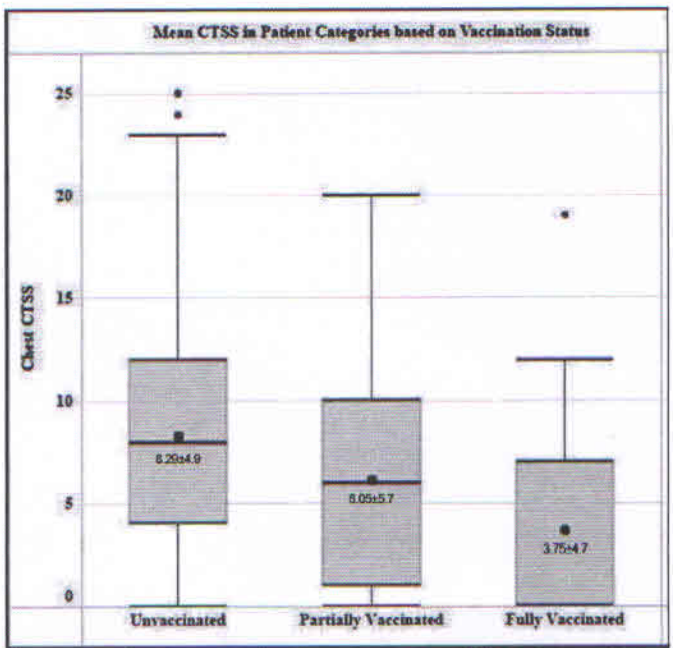

[Table/Fig-10]: Box plots showing comparison of Mean CTSS between patient categories based on vaccination status.
Blue dot within the box: Mean CTSS, Blue dots outside the box: Outliers, Black horizontal line within the box: Median CTSS.

The percentage distribution of mild, moderate and severe grades of CTSS amongst the unvaccinated, partially vaccinated and fully vaccinated groups of patients is illustrated in [Table/Fig-11]. Majority of the fully vaccinated patients (86.4%) demonstrated mild CTSS; whereas highest percentage of severe CTSS (11.5%) was reported in the unvaccinated patient group. This difference in the grades of CTSS observed in the different patient categories depending on their vaccination status, was statistically significant (p<0.01).

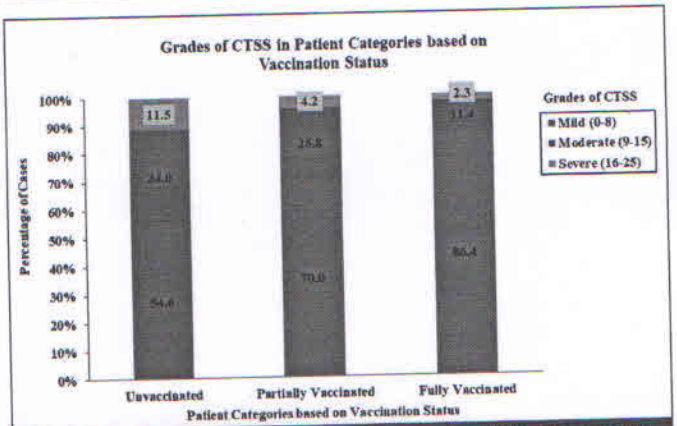

[Table/Fig-11]: Stacked column chart showing percentage distribution of grades of chest CTSS in patient categories based on vaccination status.

Association of CTSS with the two types of COVID-19 vaccines: Amongst the vaccinated cohort, 207 (88.5%) patients had received Covishield and 27 (11.5%) persons had received Covaxin. The difference between mean CTSS of patients who had received Covishield (Mean±SD:5.61±4.9) and that of patients who had received Covaxin (Mean±SD: 5.67±4.6); was statistically insignificant (p=0.954, p>0.05).

Association of CTSS with stage of lung involvement on CT: Statistically significant difference was noted in the mean CTSS among the five stages of lung involvement on CT based on the period between onset of symptoms and acquisition of CT scan (p<0.01), [Table/Fig-12].

Stages of lung involvement on CT based on the period between onset of symptoms and CT scan	Mean CTSS±SD	Number of patients
Stage 1 (0-4 days interval)	4.16±3.879	251
Stage 2 (5-9 days interval)	8.45±5.302	678
Stage 3 (10-14 days interval)	11.16±7.640	51
Stage 4 (15-21 days interval)	13.27±5.849	15
Stage 5 (>21days)	19.86±3.436	7
Total	7.66±5.645	1002

[Table/Fig-12]: Comparison of mean CTSS among stages of lung involvement on CT based on the period between symptom' onset and CT scan acquisition
p=0.0001 (p<0.01) by ANOVA test and Kruskal-Wallis Test (applied to confirm the results obtained by ANOVA)

Further, occurrence of mild grade of CTSS in majority (89.3%) of the patients belonging to the fully vaccinated cohort with no co-morbidity, was demonstrated in the two-way cross tables. None (0%) of these patients recorded severe CTSS. On the contrary, a large percentage of unvaccinated patients with co-morbidity; demonstrated either moderate or severe CTSS [Table/Fig-13].

Comorbidity status	Vaccination status	Grades of CTSS Number (N) and percentage (%) of patients			Total number of patients N=949* (100.0%)
		Mild (0-8) N=556, (58.6%)	Moderate (9-15) N=297, (31.3%)	Severe (16-25) N=96, (10.1%)	
No Co-morbidity	Unvaccinated	337 (60.6)	162 (29.1)	57 (10.3)	556 (100.0)
	Partially vaccinated	88 (75.9)	24 (20.7)	4 (3.4)	116 (100.0)
	Fully vaccinated	25 (89.3)	3 (10.7)	0 (0.0)	28 (100.0)
	Total	450 (64.3)	189 (27.0)	61(8.7)	700(100.0)
Only DM	Unvaccinated	15 (26.8)	27 (48.2)	14 (25.0)	56 (100.0)
	Partially vaccinated	14 (70.0)	4 (20.0)	2 (10.0)	20 (100.0)
	Fully vaccinated	4 (100.0)	0 (0.0)	0 (0.0)	4 (100.0)
	Total	33 (41.3)	31 (38.8)	16 (20.0)	80 (100.0)
Only HTN	Unvaccinated	21 (32.8)	35 (54.7)	8 (12.5)	64 (100.0)
	Partially vaccinated	20 (66.7)	8 (26.7)	2 (6.7)	30 (100.0)
	Fully vaccinated	5 (100.0)	0(0.0)	0(0.0)	5 (100.0)
	Total	46 (46.5)	43 (43.4)	10 (10.1)	99 (100.0)
DM+HTN	Unvaccinated	12 (30.8)	19 (48.7)	8 (10.1)	39 (100.0)
	Partially vaccinated	11 (45.8)	13(54.2)	0 (0.0)	24 (100.0)
	Fully vaccinated	4 (57.1)	2 (28.6)	1(14.3)	7 (100.0)
	Total	27 (38.6)	34 (48.6)	9 (12.9)	70 (100.0)

[Table/Fig-13]: Comorbidity* Vaccination status * Grades of CTSS -two way cross tabulation
CTSS: CT severity scores; DM: Diabetes mellitus; HTN: Hypertension;
*N=949 as Co-morbidity data was available for 949 out of 1002 study patients

Taking into account, the confounding effect of all the included independent variables, multivariate linear regression analysis showed that presence of co-morbidity and higher stage of disease were associated with higher CTSS; whereas partially/fully vaccinated patients recorded lower CTSS when compared with unvaccinated patients (adjusted R^2 is 0.230) [Table/Fig-14].

R	R^2	Adjusted R^2	Standard Error of the Estimate	Change statistics				
				R^2 Change	F Change	df1	df2	Significant F Change
0.482[c]	0.232*	0.230	4.999	0.039	47.875	1	945	0.0001
		Unstandardised Coefficients		Standardised Coefficients		t statistic		Significance
		B	Standard Error	β (Beta)				
(Constant)		1.439	0.527			2.731		0.006
Stages of lung involvement based on duration of symptoms		3.367	0.257	0.376		13.089		0.0001
Vaccination status		-2.705	0.384	-0.205		-7.046		0.0001
Comorbidity status		2.589	0.374	0.200		6.919		0.0001

[Table/Fig-14]: Multivariate regression analysis: with CTSS as a dependent variable and patient related factors such as 1) stages of lung involvement on CT based on duration of symptoms, 2) vaccination status and 3) co-morbidity status, as independent variables.
R^2: Coefficient of determination; F: F statistics; df: degrees of freedom; B: Unstandardised regression coefficient. β: Standardised regression coefficient
*R^2 is 0.232 i.e., 23.2% variation in CTSS is explained by the 3 factors: 1) stage of disease on CT chest based on symptom's duration, 2) vaccination status and 3) co-morbidity status of patients. This variation is significant with p=0.0001

DISCUSSION

In the course of evolution of the COVID-19 global pandemic, several studies have shown that various patient related factors such as age, gender, duration of symptoms, along with the number and type of co-morbidities; influence the clinical severity and outcomes of patients with COVID-19 infections [3,17-22]. Scientific literature till date has demonstrated the correlation between the clinical severity of COVID-19 disease and chest CTSS in COVID-19 patients [1-3,23-25].

Further, National SARS CoV-2 vaccination drive is underway in India as part of the global efforts to abate the onslaught of the pandemic [6]. Even so, post vaccination breakthrough infections, mainly attributable to the emergence of new variants of SARS-CoV-2 virus; are being reported all over the world, as well as in India [8,9,26,27].

In these settings, the present study assessed the association between CTSS and vaccination status in RT-PCR/RAT confirmed, symptomatic COVID-19 patients, during the second wave of the pandemic in India. The association between CTSS and clinical parameters of these patients were also investigated. Results of this study demonstrated that patients with partial and full vaccination record significantly lower mean CTSS and also report lower percentage of patients with severe grade of CTSS; when compared with the unvaccinated patient population [Table/Fig-10,11]. These results corroborated with those of previously conducted, similar Indian studies comparing chest CTSS amongst the unvaccinated and vaccinated COVID-19 patients (one of these studies was a

preprint at the time of writing this paper) [11-13]. In comparison with these studies, the present study included a larger cohort of patients.

In the present study, majority (86.4%) of the fully vaccinated patients with breakthrough infections, demonstrated mild CTSS and only 1 patient (2.3%) recorded severe CTSS. In line with previous literature reports, this data also illustrated that majority of the patients with post vaccination breakthrough infections suffer from mild disease [11-13,26,27]. All of the above mentioned results in the present study can be ascribed to the effectiveness of vaccines in preventing severe COVID-19 disease.

Patients of different age groups in the Indian population are receiving vaccines in a phased manner, as prioritisation of vaccination to the elderly population at an increased risk for developing severe COVID-19 infection; is crucial [6]. Therefore, the younger age group (18-44 years) made a sizeable contribution to the unvaccinated category (91.1%) in the current study cohort. Similar to the observations reported by previous studies, this study recorded a higher mean CTSS along with a greater percentage of patients with severe CTSS, in the middle aged (45-59 years) and elderly (>60 years) population [3,19]. One reason for this observation could be the stage of the pandemic when this study was conducted and another possible reason may be that COVID-19 infection elicits a stronger inflammatory response in the elderly population since they are more likely to have concomitant co-morbidities [19].

Higher mean CTSS and greater percentage of cases with moderate and severe grades of CTSS were seen in the male population in this study. Saeed GA et al., and Jin J-M et al., have reported in their respective studies that, men are at a higher risk of severe COVID-19 disease as compared to women and our results support their observation [3,20].

As expected, the authors of the present study found a significantly higher mean CTSS in patients with one or more co-morbidities, when compared with patients with no co-morbidities [Table/Fig-8] [21]. Also, severe CTSS was more commonly recorded in the patients with diabetes mellitus alone followed by patients with both DM and hypertension; further followed by those with hypertension alone [Table/Fig-9] [22]. Overall, these findings are in agreement with the existing literature reports that have documented the impact of co-morbidities on clinical outcomes of patients with COVID-19 [21,22]. In the current study cohort of breakthrough infections, the fully vaccinated patient with severe CTSS was 75 years of age and had co-morbidities such as diabetes and hypertension.

Pan F et al and Ding X et al in their respective studies found that the chest CT features and CT scores of patients with COVID-19, changed with duration of symptoms [17,18]. Consistent with these studies, the present study reported significantly lower mean CTSS and milder grades of CT scores in patients in the early stages of the disease. The mean CT scores were seen to progressively increase from stage 1 to stage 5.

Limitation(s)

The study cohort did not include asymptomatic and RT-PCR false negative persons; who are likely to promote spread of COVID-19 infection. Another limitation was self reporting and under reporting of co-morbidities in some of the enrolled patients. Data on obesity, ischemic heart disease, chronic renal disease and prior lung disease was not available. Details about the clinical categorisation and treatment received by the study patients were also not available. Follow-up chest CT scans were performed in some patients on the basis of clinical indication. However, such serial chest CT scans were not included in the study analysis. Further multicentric studies involving larger groups of COVID-19 patients are recommended to validate the results of this study and to evaluate the impact of SARS-CoV-2 vaccination on the overall patient outcomes.

CONCLUSION(S)

Significant association between the chest CTSS and the vaccination status, age, gender, co-morbidities and stage of disease was seen, in this large cohort of COVID-19 patients from a tertiary care diagnostic centre in Pune, Maharashtra, India. This study conducted in real world settings, reiterates that full vaccination aids in reducing the severity of lung damage in COVID-19 infections. It therefore, underscores the role played by vaccines in curbing the current COVID-19 pandemic.

Acknowledgement

The authors would like to thank Mrs. Aruna Deshpande MSc. (Statistics), for her help in statistical analysis.

REFERENCES

[1] Li K, Fang Y, Li W, Pan C, Qin P, Zhong Y et al. CT image visual quantitative evaluation and clinical classification of coronavirus disease (COVID-19). Eur Radiol. 2020;30(8):4407-16. doi: 10.1007/s00330-020-06817-6.
[2] Francone M, Iafrate F, Masci GM, Coco S, Cilia F, Manganaro L et al. Chest CT score in COVID-19 patients: correlation with disease severity and short-term prognosis. Eur Radiol. 2020;30(12):6808-17. doi:10.1007/s00330-020-07033-y.
[3] Saeed GA, Gaba W, Shah A, Al Helali AA, Raidullah E, Al Ali AB et al. Correlation between Chest CT Severity Scores and the Clinical Parameters of Adult Patients with COVID-19 Pneumonia. Radiol Res Pract. 2021;2021:6697677. doi: 10.1155/2021/6697677.
[4] Prokop M, van Everdingen W, van Rees Vellinga T, Quarles van Ufford H, Stöger L, Beenen L et al. CO-RADS: A Categorical CT Assessment Scheme for Patients Suspected of Having COVID-19-Definition and Evaluation. Radiology. 2020;296(2):E97-E104. doi: 10.1148/radiol.2020201473.
[5] Lieveld AWE, Azijli K, Teunissen BP, van Haaften RM, Kootte RS, van den Berk IAH et al. Chest CT in COVID-19 at the ED: Validation of the COVID-19 Reporting and Data System (CO-RADS) and CT Severity Score: A Prospective, Multicenter, Observational Study. Chest. 2021;159(3):1126-35. doi: 10.1016/j.chest.2020.11.026.
[6] Revised Guidelines for implementation of National COVID Vaccination Program. 2021:1-4. https://www.mohfw.gov.in/pdf/RevisedVaccinationGuidelines.pdf.
[7] Bagcchi S. The world's largest COVID-19 vaccination campaign. Lancet Infect Dis. 2021;21(3):323. doi:10.1016/S1473-3099(21)00081-5.
[8] Tyagi K, Ghosh A, Nair D, Dutta K, Singh Bhandari P, Ahmed Ansari I et al. Breakthrough COVID19 infections after vaccinations in healthcare and other workers in a chronic care medical facility in New Delhi, India. Diabetes Metab Syndr. 2021;15(3):1007-08. doi: 10.1016/j.dsx.2021.05.001.
[9] Hacisuleyman E, Hale C, Saito Y, Blachere NE, Bergh M, Conlon EG et al. Vaccine Breakthrough Infections with SARS-CoV-2 Variants. N Engl J Med. 2021;384(23):2212-18. doi: 10.1056/NEJMoa2105000.
[10] World Health Organisation. Evaluation of COVID-19 vaccine effectiveness: Interim Guidance. 2021 Mar: 1-55.
[11] P. Madhu, D. Santhosh, & Kiran Madhala. Comparison Study of Lung Involvement in Vaccinated and Un Vaccinated Covid Patients. International Journal of Health and Clinical Research. 2021;4(10):229-33.
[12] Lakhia RT, Trivedi JR . The CT Scan Lung Severity Score and Vaccination Status in COVID-19 patients in India: Perspective of an Independent Radiology Practice. medRxiv preprint doi: https://doi.org/10.1101/2021.07.15.21260597. Preprint Aug 2021.
[13] Modi SD, Shah DH, Mundhra KS, Gandhi B, Shah R, Kagathara V et al. Comparative Study of CT Severity Index and Outcome in Hospitalised Vaccinated and Non- Vaccinated Patients of Covid 19 Pneumonia. Journal of Radiology and Clinical Imaging. 2021;4(2021):93-101.
[14] Coronavirus in India: Latest Map and Case Count [Internet]. www.covid19india.org. [last updated 2021 Nov 1; cited 2022 Jan 22]. Available from: https://www.covid19india.org.
[15] India Population 2022 - Dialects, Ethnic groups, Religions, About India, Religions [Internet]. www.indiagrowing.com. [cited 2022 Jan 22]. Available from: https://www.indiagrowing.com/Maharashtra/ Pune_District/.
[16] Home [Internet]. Unique Identification Authority of India | Government of India. [last updated 2021 Dec; cited 2022 Jan 22]. Available from: https://www.uidai.gov.in/aadhaar_dashboard/.
[17] Pan F, Ye T, Sun P, Gui S, Liang B, Li L et al. Time Course of Lung Changes at Chest CT during Recovery from Coronavirus Disease 2019 (COVID-19). Radiology. 2020;295(3):715-21. doi: 10.1148/radiol.2020200370.
[18] Ding X, Xu J, Zhou J, Long Q. Chest CT findings of COVID-19 pneumonia by duration of symptoms. Eur J Radiol. 2020;127:109009. doi: 10.1016/j.ejrad.2020.109009.
[19] Chen Z, Fan H, Cai J, Li Y, Wu B, Hou Y et al. High-resolution computed tomography manifestations of COVID-19 infections in patients of different ages. Eur J Radiol. 2020;126:108972. doi: 10.1016/j.ejrad.2020.108972.
[20] Jin J-M, Bai P, He W, Wu F, Liu X-F, Han D-M et al. Gender Differences in Patients With COVID-19: Focus on Severity and Mortality. Front. Public Health. 2020;8:152. doi: 10.3389/fpubh.2020.00152.

[21] Guan WJ, Liang WH, Zhao Y, Liang HR, Chen ZS, Li YM et al. Comorbidity and its impact on 1590 patients with Covid-19 in China: A Nationwide Analysis. Eur Respir J. 2020;55(5):2000547. 2020 May 14;55(5):2000547. doi: 10.1183/13993003.00547-2020.
[22] Pal R, Bhadada SK, Misra A. COVID-19 vaccination in patients with diabetes mellitus: Current concepts, uncertainties and challenges. Diabetes Metab Syndr. Diabetes Metab Syndr. 2021;15(2):505-08. doi: 10.1016/j.dsx.2021.02.026.
[23] Ai T, Yang Z, Hou H, Zhan C, Chen C, Lv W et al. Correlation of Chest CT and RT-PCR Testing for Coronavirus Disease 2019 (COVID-19) in China: A Report of 1014 Cases. Radiology. 2020;296(2):E32-E40. doi: 10.1148/radiol.2020200642.
[24] Zhang J, Meng G, Li W, Shi B, Dong H, Su Z et al. Relationship of chest CT score with clinical characteristics of 108 patients hospitalized with COVID-19 in Wuhan, China. Respir Res. 2020;21(1):180. doi: 10.1186/s12931-020-01440-x.
[25] Colombi D, Bodini FC, Petrini M, Maffi G, Morelli N, Milanese G et al. Well-aerated Lung on Admitting Chest CT to Predict Adverse Outcome in COVID-19 Pneumonia. Radiology. 2020;296(2):E86-E96. doi: 10.1148/radiol.2020201433.
[26] Teran RA, Walblay KA, Shane EL, Xydis S, Gretsch S, Gagner A et al. Postvaccination SARS-CoV-2 infections among skilled nursing facility residents and staff members - Chicago, Illinois, December 2020-March 2021. MMWR Morb Mortal Wkly Rep. 2021;70(17):632-38.
[27] Britton A, Slifka KMJ, Edens C, Nanduri SA, Bart SM, Shang N et al. Effectiveness of the Pfizer-BioNTech COVID-19 Vaccine Among Residents of Two Skilled Nursing Facilities Experiencing COVID-19 Outbreaks — Connecticut, December 2020–February 2021. MMWR Morb Mortal Wkly Rep. 2021;70(11):396-01.

PARTICULARS OF CONTRIBUTORS:
1. Chief Radiologist, Department of Radiology, Star Imaging and Research Centre, Pune, Maharashtra, India.
2. Undergraduate Student, Government Medical College Byramjee Jeejeebhoy and Sassoon General Hospitals, Pune, Maharashtra, India.
3. Undergraduate Student, Smt. Kashibai Navale Medical College and General Hospital, Pune, Maharashtra, India.
4. Undergraduate Student, Government Medical College Byramjee Jeejeebhoy and Sassoon General Hospitals, Pune, Maharashtra, India.
5. Research Associate and Radiologist, Department of Radiology, Star Imaging and Research Centre, Pune, Maharashtra, India.
6. Founder, Star Imaging and Research Centre and Associate Professor (Honorary), Department of Radiology, B.J. Government Medical College, Pune, Maharashtra, India.

NAME, ADDRESS, E-MAIL ID OF THE CORRESPONDING AUTHOR:
Ashish Laxman Atre,
Chief Radiologist, Star Imaging and Research Centre, Deccan-Joshi Hospital Campus, Opposite Kamla Nehru Park, Erandawane, Pune, Maharashtra, India.
E-mail: atreal@gmail.com

PLAGIARISM CHECKING METHODS: [Jain H et al.]
- Plagiarism X-checker: Nov 01, 2021
- Manual Googling: Feb 15, 2022
- iThenticate Software: Mar 04, 2022 (11%)

ETYMOLOGY: Author Origin

AUTHOR DECLARATION:
- Financial or Other Competing Interests: Funded by Maharashtra Medical Research Society, Joshi Hospital, Pune, Maharashtra, India.
- Was Ethics Committee Approval obtained for this study? Yes
- Was informed consent obtained from the subjects involved in the study? Yes
- For any images presented appropriate consent has been obtained from the subjects. Yes

Date of Submission: **Oct 31, 2021**
Date of Peer Review: **Jan 07, 2022**
Date of Acceptance: **Mar 06, 2022**
Date of Publishing: **Jun 01, 2022**

B_{12} D_3 Correlation: Is Oxidative Stress a Common Link?

To the Editor:

We read with interest the article "Is there an association between vitamin B_{12} level and vitamin D status in children?" by Nalan Karabayir and colleagues, which shows evidence of an association between B_{12} and D_3 levels. We would like to congratulate the authors for introducing the topic of the relationship between these 2 apparently unconnected vitamins namely, B_{12} and D_3.

The prevalence of deficiencies of both these vitamins is quite high in adults worldwide, as well as in India as reported in various studies.[1–5] An association between D_3 and B_{12} levels has been reported in a few studies recently from Turkey in children and adolescents.[6,7]

We would like to report a similar study on adults from our institute. After ethics committee approval, we conducted a retrospective analysis of vitamin B_{12} and D_3 levels of 729 adults (male to female ratio, 308:421) between 18 and 65 years, who had undergone annual medical check-ups. B_{12} levels <200 pg/dL were found in 18.51%, whereas D3 levels <20 ng/dL were found in 53.22% of individuals. 77.03% (104/135) with B_{12} levels <200 had D_3 deficiency (<20) as compared with 47.81% (184/594) with B_{12} levels more than 200, this difference is statistically significant ($P<0.001$). Also, Spearman correlation test showed a positive association between B_{12} and D_3 levels ($r=0.277$, $P<0.001$).

This moderate-to-weak correlation could indicate a joint contribution of etiopathogenetic and socioeconomic environmental factors such as malnutrition, malabsorption, and poor exposure to sunlight resulting in deficiencies of both vitamins simultaneously.

However, the observed correlation could as well demand a biological explanation. Here, we would like to draw the attention of researchers to one more possible explanation for reduced levels of these vitamins which is, the increased consumption of both these vitamins. Indeed, oxidative stress could be the common link that escalates the consumption of both these vitamins. Vitamin D is one of the key factors in the control of inflammation and oxidative stress in humans and its deficiency is a risk factor for noncommunicable diseases.[8] Vitamin D has been shown to protect human endothelial cells from oxidative stress through the autophagic and survival pathways.[9] Furthermore, oxidative stress results in DNA damage, and B_{12} is required for DNA repair. Some evidence appears to suggest that a lower B_{12} level is related to increased pro-oxidant and decreased antioxidant status, both overall and for subclinically deficient individuals compared with those with normal B_{12} levels.[10] Thus, it may be plausible that increased oxidative stress may prove to be a constituent that ties up both these vitamins. Further studies are required to test these hypotheses. A recent study on DNA methylation in air pollution may be interesting in this regard.[11]

Narendra S. Javadekar, MD, DNB, MA*†
Abhijeet P. Joshi, DNB*
Smruti P. Pradhan, MD‡
Gauri A. Oka, MBBS, MPH§
*Department of Medicine at MMFHA Joshi Hospital
†Deenanath Mangeshkar Hospital and Research Center
‡ MMFHA Joshi Hospital and MMFHA Ratna Hospital
§Department of Research, Bharati Vidyapeeth DTU Medical College and Hospital, Pune, Maharashtra, India

REFERENCES

1. Amrein K, Scherkl M, Hoffmann M, et al. Vitamin D deficiency 2.0: an update on the current status worldwide. *Eur J Clin Nutr*. 2020;74:1498–1513.
2. Cashman KD. Vitamin D deficiency: defining, prevalence, causes, and strategies of addressing. *Calcif Tissue Int*. 2020;106:14–29.
3. Stabler SP. Clinical practice. Vitamin B12 deficiency. *N Engl J Med*. 2013;368:149–160.
4. Yajnik CS, Deshpande SS, Lubree HG, et al. Vitamin B12 deficiency and hyperhomocysteinemia in rural and urban Indians. *J Assoc Physicians India*. 2006;54:775–782.
5. Singla R, Garg A, Surana V, et al. Vitamin B12 deficiency is endemic in Indian population: a perspective from North India. *Indian J Endocrinol Metab*. 2019;23:211–214.
6. Konuksever D, Yücel Karakaya SP. Evaluation of correlation between vitamin D with vitamin B12 and folate in children. *Nutrition*. 2022;99-100:111683
7. Yetim A, Tıkız C, Baş F. Prevelance of vitamin D and B12 deficiency in adolescence. *Tuberculin Ski Test Child*. 2017;17:24–29.
8. Wimalawansa SJ. Vitamin D deficiency: effects on oxidative stress, epigenetics, gene regulation, and aging. *Biology*. 2019;8:1–15.
9. Uberti F, Lattuada D, Morsanuto V, et al. Hot topics in translational endocrinology-Emdocrine research. *J Clin Endocrinol Metab*. 2014;99:1367–1374.
10. van de Lagemaat EE, de Groot LCPGM, van den Heuvel EGHM. Vitamin B12 in relation to oxidative stress: a systematic review. *Nutrients*. 2019;11:482.
11. Yadav S, Longkumer I, Rani Garg P, et al. Association of air pollution and homocysteine with global DNA methylation: a population-based study from North India. 2021. Accessed August 19, 2021. https://doi.org/10.1371/journal.pone.0260860

The authors declare no conflict of interest.

frontiers | Frontiers in Endocrinology

TYPE Original Research
PUBLISHED 20 November 2023
DOI 10.3389/fendo.2023.1264072

OPEN ACCESS

EDITED BY
Maurizio Delvecchio,
Giovanni XXIII Children's Hospital, Italy

REVIEWED BY
Rahul Siddharthan,
Institute of Mathematical Sciences, Chennai, India
Tanja Milicic,
University of Belgrade, Serbia

*CORRESPONDENCE
Sayantan Majumdar
majumdar.sayantan@students.iiserpune.ac.in

RECEIVED 20 July 2023
ACCEPTED 17 October 2023
PUBLISHED 20 November 2023

CITATION
Majumdar S, Kalamkar SD, Dudhgaonkar S, Shelgikar KM, Ghaskadbi S and Goel P (2023) Evaluation of HbA1c from CGM traces in an Indian population. *Front. Endocrinol.* 14:1264072. doi: 10.3389/fendo.2023.1264072

Evaluation of HbA1c from CGM traces in an Indian population

Sayantan Majumdar[1]*, Saurabh D. Kalamkar[2], Shashikant Dudhgaonkar[3], Kishor M. Shelgikar[4], Saroj Ghaskadbi[2] and Pranay Goel[1]

[1]Department of Biology, Indian Institute of Science Education and Research Pune, Pune, Maharashtra, India, [2]Department of Zoology, Savitribai Phule Pune University, Pune, Maharashtra, India, [3]Health Centre, Savitribai Phule Pune University, Pune, Maharashtra, India, [4]Department of General Medicine, Joshi Hospital, Pune, Maharashtra, India

Introduction: The development of continuous glucose monitoring (CGM) over the last decade has provided access to many consecutive glucose concentration measurements from patients. A standard method for estimating glycated hemoglobin (HbA1c), already established in the literature, is based on its relationship with the average blood glucose concentration (aBG). We showed that the estimates obtained using the standard method were not sufficiently reliable for an Indian population and suggested two new methods for estimating HbA1c.

Methods: Two datasets providing a total of 128 CGM and their corresponding HbA1c levels were received from two centers: Health Centre, Savitribai Phule Pune University, Pune and Joshi Hospital, Pune, from patients already diagnosed with diabetes, non-diabetes, and pre-diabetes. We filtered 112 data-sufficient CGM traces, of which 80 traces were used to construct two models using linear regression. The first model estimates HbA1c directly from the average interstitial fluid glucose concentration (aISF) of the CGM trace and the second model proceeds in two steps: first, aISF is scaled to aBG, and then aBG is converted to HbA1c via the Nathan model. Our models were tested on the remaining 32 data-sufficient traces. We also provided 95% confidence and prediction intervals for HbA1c estimates.

Results: The direct model (first model) for estimating HbA1c was $HbA1c_{mmol/mol} = 0.319 \times aISF_{mg/dL} + 16.73$ and the adapted Nathan model (second model) for estimating HbA1c is $HbA1c_{mmol/dL} = 0.38 \times (1.17 \times ISF_{mg/dL}) - 5.60$.

Discussion: Our results show that the new equations are likely to provide better estimates of HbA1c levels than the standard model at the population level, which is especially suited for clinical epidemiology in Indian populations.

KEYWORDS

continuous glucose monitoring (CGM), glycated hemoglobin (HbA1c), type 2 diabetes (T2D), average blood glucose concentration (aBG), average interstitial fluid glucose concentration (aISF)

10.3389/fendo.2023.1264072

1 Introduction

Type 2 diabetes mellitus (T2D) is one of the most common metabolic disorders in India. Understanding the metabolic pathways and mechanisms involved in the development of T2D in patients play an important role in its diagnosis and treatment. Traditionally, it involves measuring the fasting blood glucose concentration (FBG) and postprandial blood glucose concentration (PPBG). Since the late 1970s, there have been reports of a correlation between HbA1c and blood glucose concentration (BG), and that HbA1c could be a useful tool for long-term BG control. Gabbay et al. (1) studied the correlation between HbA1a, HbA1b, and HbA1c with 24-hour urinary glucose concentration collected over periods of 1, 2, and 3 months for 220 diabetic patients and suggested that glycosylated hemoglobin could act as a good index for long-term BG levels in people with T2D. Santiago et al. (2) further studied the correlation between HbA1c and PPBG. Clarke et al. (3) showed that HbA1c is correlated with aBG over 2 months, and therefore, is a good index for aBG and is a useful tool for understanding the quality of BG control in a patient. Lecomte et al. (4) also confirmed in a group of 138 patients that HbA1c is a good index for BG control. Distiller (5) compared the efficacy of PPBG and HbA1c as indices for BG control and showed that HbA1c is a significantly better index.

There is a plethora of other new metrics being developed to understand the glycemic state of the patient, such as time in range (TIR). HbA1c is one of the most reliable metrics for understanding long-term BG changes in a patient. Therefore, accurate experimental methods (6) have been developed to measure HbA1c levels. However, with the development of flash glucose monitoring (FGM) and eventually CGM technologies, clinicians now have access to many consecutive interstitial fluid glucose concentration (ISF) measurements (CGM traces). This encouraged the development of methods for estimating metrics such as FGM, PPBG, TIR, and HbA1c from the CGM traces.

Sikaris (7) showed that although for a single measurement HbA1c and BG had been shown to be correlated, including multiple measurements like CGM traces improved the correlation further. They concluded that not only was estimating HbA1c from the HbA1c–BG relationship viable, but also that it would become the standard method of estimating HbA1c. Mazze (8) also showed that BG from self-monitoring blood glucose (SMBG) and CGM traces were highly correlated, and that the HbA1c estimates obtained using them were not significantly different, although different patterns of SMBG and CGM traces could produce the same HbA1c. This suggests that HbA1c is a metric that can be reliably estimated. Nathan et al. (9) used linear regression to estimate aBG from HbA1c levels at the population level. This relationship has been used to develop a method for estimating HbA1c levels from aBG. This method was adopted as the standard for obtaining HbA1c estimates (10). This method was also used to estimate HbA1c values using the Abbot Libre FreeStyle Pro device for the CGM report generated by the device.

In recent years, after Nathan et al. (9) published their method, many similar methods have been developed for estimating HbA1c. Kovatchev et al. (11) provided a dynamic method for accurately estimating average HbA1c using regular SMBG readings for T2D patients. The method was later validated in patients with type 1 diabetes (T1D) and showed similar performance (12). Beck et al. (13) showed that experimentally measured HbA1c alone cannot be reliably used as a metric for glycemic control in an individual. They suggested that the glucose profile from the CGM trace and aBG calculated from the CGM trace were also considered. They also provided a method for estimating HbA1c from a given CGM trace and suggested that estimated HbA1c should also be considered as a metric for an individual's glycemic control. Fan et al. (14) had established a relationship between HbA1c and FBG and PPBG which are both categorized as SMBG. They also provided a method for estimating HbA1c but also showed that FBG and HbA1c levels are strongly correlated.

Bergenstal et al. (15) renamed the estimated HbA1c as the glucose management indicator (GMI), a metric for glycemic control and management. They also provided a new method for estimating GMI from a given CGM trace. The model was then validated by Leelarathna et al. (16) using guardian 3 and navigator 2 sensor data. Perlman et al. (17) however showed that there can be a substantial difference between experimentally measured HbA1c and GMI values for T1D patients especially, with patients having advanced chronic kidney disease. Shah et al. (18) also showed that it does not correlate well with HbA1c for non-diabetic patients. Estimated HbA1c is increasingly being replaced by GMI, which is used as a metric for glycemic control. Therefore, attempts to improve GMI to closely reflect HbA1c levels and be a reliable metric for glycemic control are an active field of research.

Recently, Oriot and Hermans (19) showed that HbA1c values were overestimated using Nathan's equation from CGM traces obtained using the Free Style Libre device for T1D patients. This contrasts with Hu et al. (20), who showed that HbA1c estimated using Nathan's equation on CGM traces obtained by FreeStyle Libre underestimated the experimental HbA1c values. Hu et al. (20) also produced a total of seven models, based on linear and nonlinear regression analysis for estimating HbA1c values from a given CGM trace. These reliability issues of GMI or estimated HbA1c indicate that there is still a need for a new method for estimating HbA1c from a given CGM trace for an individual that works for all pre-diabetic, diabetic, and non-diabetic groups. Xu et al. (21) suggested a kinetic model for estimating HbA1c and showed that it provides a highly accurate estimate of HbA1c. He also improved the kinetic model to include the life-cycle of the red blood cells (RBC) containing the HbA1c molecules (22).

We show that the HbA1c estimates obtained using Nathan's equation are not statistically reliable for the Indian population, and we provide two new methods for estimating HbA1c.

2 Materials and methods

2.1 Subject recruitment and measurement of blood biochemical parameters

A CGM dataset containing traces of 50 participants was collected at the Primary Care Health Centre, Savitribai Phule Pune University, Pune. For each participant, a FreeStyle Libre Pro

10.3389/fendo.2023.1264072

CGM sensor (Abbott, UK) was inserted subcutaneously on the back of the upper arm by Dr. Shashikant Dudhgaonkar at the Health Centre, Savitribai Phule Pune University, Pune, India, between July 2021 and September 2021. This factory-calibrated glucose sensor recorded subcutaneous ISF every 15 min for 14 days. All participants were advised to continue their normal diet and exercise routine. On the 14th day, the CGM device was removed, and the data were downloaded and analyzed using FreeStyle Libre Pro software. The CGM devices were provided to the participants through the Rastriya Ucchattar Shiksha Abhiyan (RUSA) grant from Savitribai Phule Pune University. We refer to this dataset as the Pune-2021 dataset.

The CGM data collected in the Pune-2021 dataset were then filtered into two sets: a *data-sufficient* Pune-2021 dataset and a *data-insufficient* Pune-2021 dataset in the following way. Data sufficiency was checked according to (i) the number of days the sensor was active, and (ii) the percentage of measurements recorded, as suggested by Danne et al. (10): From the measurement ID provided in the CGM trace data file, the number of ISF measurements, N, recorded by the device was calculated. The timestamps provided in the CGM trace were used to calculate the effective number of days, n_d for which the CGM device was active. However, this number was rounded off to the nearest integer using the `round` function provided by the `NumPy` package (23). The percentage of measurements recorded by the device was calculated using Δt_m, which is the time difference in seconds between the first and last readings. Δt_m was used to calculate the total number of readings recorded by the device as $N_{total} = \lfloor \frac{\Delta t_m}{60\times 15} \rfloor + 1$. The percentage of measurements was calculated as $N_p = 100 \times N/N_{\text{total}}$. If $n_d \geq 14$ and $N_p \geq 70\%$ for a given CGM trace, we categorized the CGM trace as data-sufficient; otherwise, it was categorized as data-insufficient.

After the data-insufficient CGM traces were filtered out, 12 pre-diabetic, 13 diabetic, and 14 non-diabetic CGM traces remained and were categorized as data-sufficient.

A second dataset of 78 CGM traces along with their HbA1c levels (by HPLC) was collected by Dr. K. M. Shelgikar at the Tertiary Care Center, Joshi Hospital, Shivaji Nagar, Pune from 2018 to 2020. Data were collected as part of routine patient care and anonymized for analysis. This dataset is referred to as the Joshi-2018 dataset. Similar to the Pune-2021 dataset, the Joshi-2018 dataset was filtered as data-sufficient and data-insufficient subsets. After filtering out the data-insufficient CGM traces from the Joshi-2018 dataset, only 73 CGM traces were considered as data sufficient.

The complete CGM-dataset, including both the Pune-2021 dataset and the Joshi-2018 dataset, contained the CGM traces and the corresponding HbA1c levels of 128 participants, 15 of whom were pre-diabetic, 94 were diabetic, and 19 were non-diabetic. The data-sufficient subset of the CGM-dataset contained 112 CGM traces, of which 12 were pre-diabetic, 86 were diabetic, and 14 were non-diabetic. A sample of 32 data-sufficient CGM traces and their corresponding HbA1c measurements was separated as a test set for validation purposes; the remaining 80 data-sufficient CGM traces were grouped as the training CGM-dataset. The complete CGM-dataset including the data-insufficient CGM traces was used to validate the HbA1c estimates obtained using the Nathan model (9) but only the data-sufficient CGM traces of the training CGM-dataset were used to construct our models, which were then validated using the data-sufficient CGM traces of the test CGM-dataset.

2.2 Comparing Nathan HbA1c estimates with experimentally measured HbA1c

Nathan et al. (9) collected a dataset of 2,700 glucose measurements from 268 T1D patients, 159 T2D patients, and 80 non-diabetic participants. Their dataset contained CGM traces and finger-stick measurements that were collected as different measures of glycemia.

The ISF measurements were scaled by a factor of 1.05 to estimate the corresponding BG. aBG was calculated by taking the weighted average of all the blood glucose concentration measurements collected. All measurements in a day were given equal weights, which were inversely proportional to the number of measurements taken on that day. The aBG was calculated by taking the mean of all measurements, giving the measurements on each day an equal weight. The expression to obtain the aBG is

$$\text{aBG} = \frac{1}{(m_1+m_2)}\left\{\sum_{i=1}^{i=m_1}\left(\frac{1}{n_{1,i}}\right)\text{BG}_i + \sum_{i=1}^{i=m_2}\left(\frac{1}{n_{2,i}}\right)(1.05\times \text{ISF}_i)\right\}, \tag{1}$$

where aBG represents the average blood glucose concentration, BG_i is the ith SMBG measurements, ISF_i is the ith CGM measurement, m_1 and m_2 are the number of SMBG and CGM measurements respectively, $n_{1,i}$ is the number of SMBG measurements taken on the day BG_i was taken, and $n_{2,i}$ is the number of CGM measurements taken on the day ISF_i was taken.

A linear regression analysis was performed by Nathan et al. (9) taking the calculated aBG as the dependent variable and the HbA1c as the independent variable and obtained this relation:

$$aBG_{mg/dL} = 28.7 \times HbA1c_{\%} - 46.7, \tag{2}$$

(2) can also be written as:

$$\text{HbA1c}_{\%} = \frac{1}{28.7}\{46.7 + (1.05\times \text{aISF}_{mg/dL})\}, \tag{3}$$

$$= 1.627 + 0.035\times(1.05\times \text{aISF}_{mg/dL}), \tag{4}$$

$$\text{HbA1c}_{mmol/mol} = 0.38\times(1.05\times \text{aISF}_{mg/dL}) - 5.60, \tag{5}$$

to relate HbA1c and aISF directly.

We used a paired t-test to verify whether the two groups, that is, the experimentally measured HbA1c from the CGM-dataset and the corresponding HbA1c calculated using the Nathan model Eq. (5), and Eq. (1), are statistically indistinguishable. Calculations were performed using the `ttest_rel` function of the `stats` module of the `SciPy` package (24). Similarly, a paired t-test was performed with only the data sufficient (including both the training and test datasets) CGM traces from the CGM dataset.

2.3 Direct model

To directly construct a model between aISF and HbA1c, we assumed a linear relationship and performed a regression analysis. Note that the aISF here is an equally weighted average of all the ISF measurements in a given CGM trace,

$$\text{aISF}_{mg/dL} = \frac{1}{N}\sum_{i=1}^{i=N}\text{ISF}_{i,mg/dL}, \tag{6}$$

where $\text{aISF}_{mg/dL}$ represents the calculated aISF in mg/dL, $\text{ISF}_{i,mg/dL}$ represents the ith ISF measurement from the given CGM trace in mg/dL and N represents the total number of measurements in the given CGM trace. The linear regression equation for the direct model is

$$HbA1c_{mmol/mol} = \beta_1 \times aISF_{mg/dL} + \beta_0, \tag{7}$$

where $\text{aISF}_{mg/dL}$ represents the aISF in mg/dL, $\text{HbA1c}_{mmol/mol}$ represents the HbA1c in mmol/mol, β_1 the slope in mmoldL/(molmg) and β_0 the intercept in mmol/mol.

We obtained the ordinary least square (OLS) estimates $\hat{\beta}_0$ and, $\hat{\beta}_1$ of the parameters β_0 and, β_1. We also calculated the 95% confidence interval for $\hat{\beta}_0$ and $\hat{\beta}_1$ along with 95% confidence interval and the 95% prediction interval of HbA1c for any given aISF. This analysis was performed using the `LinearRegression` function from the `linear_model` module of the `scikit-learn` package (25). However, the confidence and prediction intervals were calculated using the standard OLS solution formulae.

A paired t-test was then performed on the HbA1c estimated using the direct model and the experimental values for the data-sufficient CGM traces from the test CGM-dataset to verify whether the HbA1c estimates obtained using $\hat{\beta}_0$ and $\hat{\beta}_1$ were statistically indistinguishable from the experimental HbA1c value at the population level. The t-test was performed using the `ttest_rel` function of the `stats` module of the `SciPy` package.

We also used the training dataset of CGM traces and calculated the 5-fold cross validation root mean squared error (RMSE) to validate the 95% confidence interval for the direct model.

2.4 Adapted Nathan model

In *Section 2.3*, we constructed a linear model for estimating HbA1c from the aISF calculated from a given CGM trace. Although such a relationship, if reliable, can be valuable, it requires us to base our HbA1c estimates on the ISF values. Traditionally, however, for the diagnosis of T2D and analysis of the glycemic state of an individual, various metrics such as FBG, PPBG, and HbA1c have always been based on BG. The current CGM devices, however, report ISF readings, and therefore, to use these CGM traces with our current diagnostic methods, it is important to develop a reliable method for converting the ISF readings to their corresponding BG readings. The ISF measurements in the CGM traces of the dataset used by Nathan et al. (9) were scaled to their BG values using a scaling factor of 1.05. We suspected that obtaining a better estimate of this scaling factor would improve HbA1c estimates.

Therefore, we constructed a linear model for estimating HbA1c from the calculated aISF [aISF was constructed using Eq. (6)] via the aBG. We considered a model in which we estimated aBG by scaling aISF by a factor of ω and used Eq. (2) to obtain the estimate of HbA1c. This model represented by Eq (8). is

$$HbA1c_{mmol/mol} = 0.38 \times (\omega \times aISF_{mg/dL}) - 5.60, \tag{8}$$

where $\text{aISF}_{mg/dL}$ represents the aISF in mg/dL, $\text{HbA1c}_{mmol/mol}$ represents the HbA1c in mmol/mol and, ω the scaling factor. Now, Eq. (8) can also be written as:

$$\frac{HbA1c_{mmol/mol} + 5.60}{0.38} = (\omega \times aISF_{mg/dL}), \tag{9}$$

The OLS solutions for the estimate $\hat{\omega}$, of the coefficient ω are the same for both Eqs. (8) and (9).

We obtain the OLS estimate $\hat{\omega}$ using Eq. (9), where we took the calculated $\text{aISF}_{mg/dL}$ as the independent variable and the transformed experimental HbA1c values, $\frac{HbA1c_{mmol/mol}+5.60}{0.38}$, as the dependent variable. The analysis was performed using the `LinearRegression` function from the `linear_model` module of the `scikit-learn` package. Data-sufficient CGM traces and their corresponding HbA1c values from the training CGM dataset were used for this analysis. We calculated the 95% confidence interval for $\hat{\omega}$, the 95% confidence interval and 95% prediction interval for estimated HbA1c corresponding to an aISF calculated from any CGM trace. These intervals were calculated using standard OLS solution formulae for constrained linear regression.

A paired t-test was performed with the HbA1c estimates made using the adapted Nathan model and the experimentally measured HbA1c values for the data-sufficient traces of the test CGM-dataset, using the `ttest_rel` function from the `stats` module of the `SciPy` package to confirm that the HbA1c estimates from the adapted Nathan model were not significantly different from the experimental HbA1c values at the population level.

Finally, using the training CGM-datset a 5-fold cross validation RMSE was calculated for the adapted Nathan model to validate the reliability of the 95% confidence intervals of the adapted Nathan model.

3 Results

We show that the mean of the estimates provided by the standard Nathan et al. (9) method for HbA1c at the population level is not statistically reliable with respect to the experimental HbA1c values for an Indian population. Next, we provide the results for the direct model and the adapted Nathan model based on OLS linear regression for estimating HbA1c from a given CGM trace. We provide the 95% confidence interval for the two models and the 95% prediction intervals for the HbA1c estimates of these two models, which are visualized in Figures 1, 2, showing the three models for estimating HbA1c along with the 95% confidence interval (Figure 1) and the 95% prediction interval (Figure 2). We also provide a user-friendly web app for academic use, CGM Analyzer [version 0.1] (https://digimed.acads.iiserpune.ac.in/fgm-

10.3389/fendo.2023.1264072

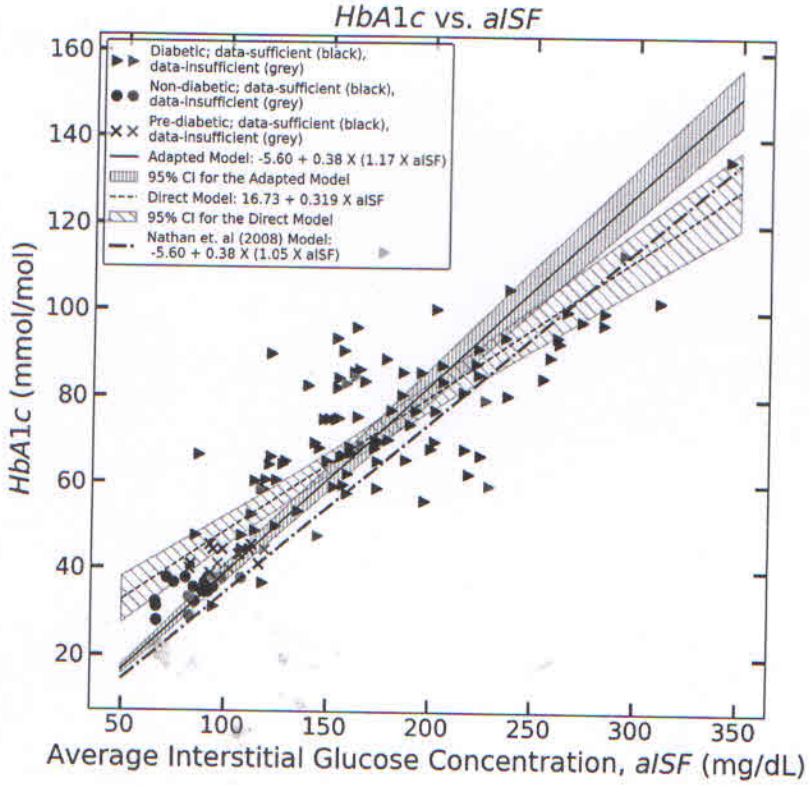

FIGURE 1
The figure represents the experimentally measured HbA1c and aISF values (calculated as described in *Section 2.3*) of the CGM dataset. The pre-diabetic participants are represented by crosses, diabetic participants are represented by solid triangles and non-diabetic participants are represented by solid circles. The scatter points representing participants with a data-sufficient CGM trace [according to Danne et al. (10)] are colored black, whereas the participants with a data-insufficient CGM trace are colored gray. The solid black line and the corresponding hatched region represent Eq. (11), which the 95% confidence interval, and the dashed line along with its corresponding hatched region, represents Eq. (10) and its corresponding 95% confidence interval. The dotted dash line represents Eq. (5).

tools), created using MATLAB R2022a. The HbA1c estimates along with their 95% prediction intervals can be calculated for a given CGM trace.

3.1 Coefficient estimates for the direct model

The paired t-test was performed using the CGM traces of the complete CGM-dataset between the experimental HbA1c values and the corresponding Nathan HbA1c estimates calculated using Eqs (1). and (5) generated a p-value<0.001. Similarly, a paired t-test with data-sufficient CGM traces from the CGM-dataset also generated a p-value of<0.001. Considering $\alpha = 0.05$, the Nathan model-estimated HbA1c values, both for data-sufficient and data-insufficient CGM traces, were significantly different from the corresponding experimentally measured HbA1c values for the Indian population.

This led us to construct a direct model for estimating HbA1c levels from aISF. We performed a linear regression analysis to establish a relationship between aISF and HbA1c using the data-sufficient CGM traces of the training CGM dataset. We obtained an estimate of the coefficient β_0 of the model, Eq. (7), $\hat{\beta}_0 = 16.73$ $mmol/mol$, with a 95% confidence interval of [9.39 mmol/mol, 24.07 mmol/mol] and an estimate for β_1, $\hat{\beta}_1 = 0.319$ $mmol\ dL/(molmg)$ with a 95% confidence interval of [0.274 mmol dL/(molmg), 0.363 mmol dL/(molmg)]. The analysis yielded Eq. (10), with an $R^2 = 0.726$ and a *p-value* <0.01. Therefore, the direct model, Eq. (7) with the estimates $\hat{\beta}_0$ and $\hat{\beta}_1$ is given by

$$HbA1c_{mmol/mol} = 0.319 \times aISF_{mg/dL} + 16.73, \quad (10)$$

where $aISF_{mg/dL}$ represents the aISF in mg/dL, and $HbA1c_{mmol/mol}$ represents HbA1c in mmol/mol. Figure 1, shows Eq. (10) as the black dashed line along with the 95% confidence interval for $HbA1c_{mmol/mol}$, corresponding to any $aISF_{mg/dL}$ calculated from a given CGM trace. The formulae for obtaining the 95% confidence and prediction interval for any HbA1c estimate are provided in the Supplementary Material. The 95% prediction interval width calculated for the HbA1c estimates was on the order of 48.50 mmol/mol.

3.2 Coefficient estimates of the adapted Nathan model

We constructed a direct model, given by Eq. (10) to estimate HbA1c from the aISF for any given CGM trace. However, we suspect that the model described in Eq. (8), where HbA1c was estimated from a

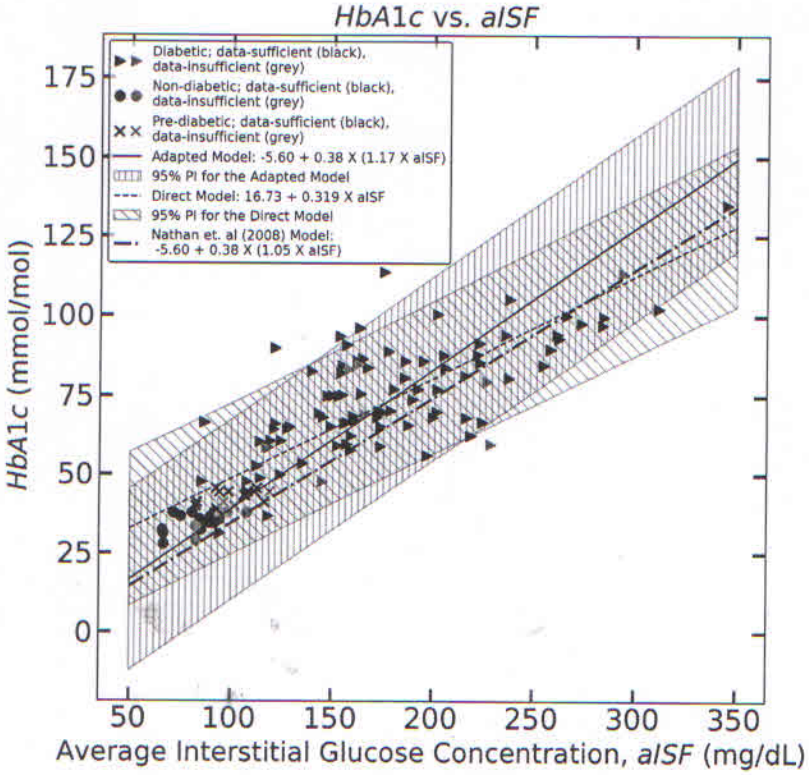

FIGURE 2
The figure represents the experimentally measured HbA1c and aISF values (calculated as described in *Section 2.3*) of the CGM dataset. The pre-diabetic participants are represented by crosses, diabetic participants are represented by solid triangles and, non-diabetic participants are represented by solid circles. The scatter points representing participants with a data-sufficient CGM trace [according to Danne et al. (10)] are colored black, whereas the participants with a data-insufficient CGM trace are colored gray. The solid black line and the corresponding hatched region represent Eq. (11), which the 95% prediction interval, and the dashed line, along with its corresponding hatched region, represents Eq. (10) and its corresponding 95% prediction interval. The dotted dash line represents Eq. (5)

scaled aISF value using Eq. (2) would provide better estimates of HbA1c levels. The OLS solution for linear regression analysis using Eq. (9), while keeping the intercept zero, would provide us with an estimate of the scaling factor for obtaining aBG from aISF.

The estimation of the scaling factor in Eq. (9), $\hat{\omega}$, obtained using the `LinearRegression` function of the `scykit-learn` package with the intercept set to zero, on the data-sufficient training CGM-dataset, is $\hat{\omega} = 1.17$, with a 95% confidence interval (1.12, 1.22). The analysis yielded an $R^2 = 0.595$ and, a *p-value*<0.01. The estimate, $\hat{\omega}$, obtained using the analytical solution for obtaining the OLS estimate of ω from Eq. (8) yields an identical result. The equation for obtaining HbA1c estimates using the adapted Nathan model is represented by Eq. (11) below

$$HbA1c_{mmol/dL} = 0.38 \times (1.17 \times aISF_{mg/dL}) - 5.60, \quad (11)$$

where $aISF_{mg/dL}$ represents the aISF in mg/dL, and $HbA1c_{mmol/mol}$ represents HbA1c in mmol/mol. Figure 1 shows Eq. (11) as a solid black line, along with the 95% confidence interval for $HbA1c_{mmol/mol}$ corresponding to any $aISF_{mg/dL}$. The formulae for obtaining the confidence and prediction intervals for any HbA1c value estimated using Eq. (11) are provided in the Supplementary Material. The 95% prediction interval width calculated for the HbA1c estimates are in the order of 57.87 mmol/mol.

3.3 Validation of the direct and adapted models

In *Sections 3.1 and 3.2*, we constructed two models for estimating HbA1c from the aISF calculated from any given CGM trace. We then constructed 95% prediction intervals for HbA1c estimates calculated using the models. The formulae for constructing the prediction interval corresponding to any estimated HbA1c level for both models are provided in the Supplementary Material.

A paired t-test performed between the experimentally measured HbA1c from the test CGM-dataset and the HbA1c estimates obtained from their corresponding CGM trace using the direct model generates a p-value of 0.643 and using the adapted Nathan model it generates a p-value of 0.715. This indicates that at the population level, the HbA1c estimates for an independent sample of CGM traces were statistically ($\alpha = 0.05$) indistinguishable from the experimental HbA1c. The 5-fold cross validation root mean squared error (RMSE) for the HbA1c estimates obtained using the direct model on the training CGM-datasets is 11.9 mmol/mol and for the estimates obtained using the adapted Nathan model it is 14.3 mmol/mol. The 95% confidence interval for the direct model was on the order of 9.48 mmol/mol and for the adapted Nathan model the 95% confidence interval was on the order of 7.70 mmol/mol.

A t-test performed using the Nathan model HbA1c estimates for the test CGM-dataset generated a p-value<0.01, indicating that at the population level, the Nathan model HbA1c estimates were statistically different from the experimental value (taking $\alpha = 0.05$).

4 Discussion

The development of CGM technology provides a large number of glucose concentration measurements. This provides a great opportunity to study the glucose dynamics and glycemic state of an individual. The current CGM devices, however, only provide ISF measurements, while traditionally it has been the norm to study glucose dynamics with BG measurements. Therefore, a large bulk of our understanding of glucose dynamics, glycemic states, and metabolic diseases, such as diabetes, is based on BG values. To use the CGM traces provided by these devices, it is important to reliably estimate the corresponding BG, especially HbA1c, from any given CGM trace. Typically, regression estimates are used to relate the average glucose level from the CGM to HbA1c. Bailey et al. (26) showed that a 7-day CGM trace provides a satisfactory estimate of GMI or estimated HbA1c comparable to estimates obtained from 14-day CGM.

The analyses conducted by Nathan et al. (9), Hu et al. (20), Bergenstal et al. (15), and Xu et al. (21) used large CGM trace datasets and their corresponding HbA1c values. While these are important estimates, it is equally important to ask if these models continue to be applicable to different populations. Indeed, it has been shown that regression equations vary with ethnicity; for instance, Hu et al. (20) and Oriot and Hermans (19) cite over- or underestimation relative to the Nathan model. To the best of our knowledge, no major study has validated these estimates in an Indian population.

We used a dataset of 128 CGM traces collected from an Indian population, sorted to use only data-sufficient CGM traces to construct models suitable for this population. We showed that the standard method of estimating HbA1c using Nathan's equation does not provide a statistically reliable estimate. Therefore, we suggest two new methods for estimating HbA1c that are better suited to the Indian population. The direct method for estimating HbA1c from ISF values, as described in *Section 2.3*, provides an estimate along with a 95% confidence and prediction interval for the estimate given an aISF value. The mean HbA1c estimates provided by the direct model were statistically indistinguishable from the mean experimental HbA1c measurement for the data-sufficient test CGM-dataset. Furthermore, we suspected that the inclusion of an improved method of estimating BG from ISF could improve the estimates provided by Eq. (5). Therefore, in *Section 3.2*, we constructed a new linear model for estimating BG from ISF using linear regression. The mean HbA1c estimates provided by this method were indistinguishable from the mean experimentally measured HbA1c values of the data-sufficient test CGM-dataset. However, the 95% prediction interval was large. We showed that the mean HbA1c estimates obtained using these two models, the direct model, and the adapted Nathan model, were not significantly different from the mean experimental HbA1c. However, the mean experimental HbA1c level was significantly different from the mean estimates provided by the Nathan model at the population level.

From the analysis of the model performance on the test CGM-dataset, we can conclude that although our models for estimating HbA1c provide a wide 95% prediction interval, which includes the HbA1c estimates obtained using the Nathan model, the mean HbA1c estimates provided by our models at the population level are statistically indistinguishable from the mean experimental HbA1c values, unlike the HbA1c estimates obtained using the Nathan model. This shows that the direct and adapted Nathan models can provide a more reliable HbA1c estimate than the Nathan model can. Such estimates are valuable at the population level, as in clinical epidemiological studies.

The strength of thsi study is that it is the first investigation of its kind in an Indian population. Furthermore, we outline that there are subtleties in the estimation procedure; depending on the question of interest, these lead to alternate formulations of the problem. We applied both approaches to the same dataset, which made it easier to compare the two methods. The weakness of our study is that the dataset was limited, and the results should be seen as prospective. We hope that future studies will test these hypotheses with greater statistical power.

Because the computed prediction intervals are rather wide, we claim that none of the models described above are suitable for estimating HbA1c in individuals with (clinical) reliability. This raises a deeper question: Can individual HbA1c estimates be obtained using only aISF values calculated from a CGM trace? Or does it require knowledge of some additional information regarding the individual not contained in their CGM? That is, it remains an open question although ISF and BG are highly correlated with HbA1c, why are the models unable to provide tighter estimates of HbA1c from aISF or aBG values alone?

Data availability statement

The raw data supporting the conclusions of this article will be made available by the authors, without undue reservation.

Ethics statement

The study protocol for the Pune-2021 dataset was approved by the Institutional Ethical Committee (IEC) of Savitribai Phule Pune University, Pune, India (SPPU/IEC/2020/102). The study protocol for the Joshi-2018 dataset was approved by the IEC of Maharashtra Medical Research Society (ECR/311/Inst/MH/2013/RR-19; Dated 14 March 2023). Informed consent from all participants was collected prior to their participation in the studies. The data analysis was reviewed and approved by the Institutional Human Ethics Committee (IHEC) of IISER Pune (IHEC/Admin/2021/015).

Author contributions

SM: Software, Visualization, Writing – original draft, Methodology. SK: Data curation, Writing – review & editing, Investigation. SD: Data curation, Writing – review & editing, Investigation. KS: Data curation, Writing – review & editing, Investigation. SG: Data curation, Funding

acquisition, Project administration, Writing – review & editing, Conceptualization, Investigation, Supervision. PG: Supervision, Writing – original draft, Writing – review & editing, Methodology, Conceptualization.

Funding

The author(s) declare that financial support was received for the research, authorship, and/or publication of this article. This work was financially supported by Rastriya Ucchattar Shiksha Abhiyan (RUSA CBS TH 4.3), Savitribai Phule Pune University, Pune. SK is a recipient of a Senior Research Fellowship from the Council of Scientific and Industrial Research (CSIR), India. SM is a Junior Research Fellow supported by a DST INSPIRE Fellowship, Department of Science and Technology, Government of India.

Acknowledgments

We thank all study subjects for their participation in this study. We acknowledge the financial help from all funding agencies mentioned.

Conflict of interest

The authors declare that the research was conducted in the absence of any commercial or financial relationships that could be construed as a potential conflict of interest.

Publisher's note

Supplementary material

The Supplementary Material for this article can be found online at: https://www.frontiersin.org/articles/10.3389/fendo.2023.1264072/full#supplementary-material

References

1. Gabbay KH, Hasty K, Breslow JL, Ellison RC, Bunn HF, Gallop PM. Glycosylated hemoglobins and long-term blood glucose control in diabetes mellitus. *J Clin Endocrinol Metab* (1977) 44:859–64. doi: 10.1210/jcem-44-5-859

2. Santiago JV, Davis J, Fisher F. Hemoglobin a1c levels in a diabetes detection program. *J Clin Endocrinol Metab* (1978) 47:578–80. doi: 10.1210/jcem-47-3-578

3. Clarke J, Passa P, Canivet J. Hba1c: need of its dosage in diabetics (author's transl). *La Nouvelle Presse Medicale* (1979) 8:513–7.

4. Lecomte M, Schoos R, Schoos-Barbette S, Luyckx A, Lambotte C, Lefebvre P. Hemoglobin a1c and diabetes control (author's transl). *Diabete Metabolisme* (1979) 5:57–61.

5. Distiller LA, Zail SS. The use of glycosylated haemoglobin measurements in the control of the diabetic patient. *South Afr Med J* (1979) 55:335–7.

6. Davis J, Mcdonald JM, Jarett L. A high-performance liquid chromatography method for hemoglobin a1c. *Diabetes* (1978) 27:102–7. doi: 10.2337/diab.27.2.102

7. Sikaris K. The correlation of hemoglobin a1c to blood glucose. *J Diabetes Sci Technol* (2009) 3:429–38. doi: 10.1177/193229680900300305

8. Mazze R. The future of self-monitored blood glucose: mean blood glucose versus glycosylated hemoglobin. *Diabetes Technol Ther* (2008) 10:S–93. doi: 10.1089/dia.2008.0006

9. Nathan DM, Kuenen J, Borg R, Zheng H, Schoenfeld D, Heine RJ, et al. Translating the a1c assay into estimated average glucose values. *Diabetes Care* (2008) 31:1473–8. doi: 10.2337/dc08-0545

10. Danne T, Nimri R, Battelino T, Bergenstal RM, Close KL, DeVries JH, et al. International consensus on use of continuous glucose monitoring. *Diabetes Care* (2017) 40:1631–40. doi: 10.2337/dc17-1600

11. Kovatchev BP, Flacke F, Sieber J, Breton MD. Accuracy and robustness of dynamical tracking of average glycemia (a1c) to provide real-time estimation of hemoglobin a1c using routine self-monitored blood glucose data. *Diabetes Technol Ther* (2014) 16:303–9. doi: 10.1089/dia.2013.0224

12. Kovatchev BP, Breton MD. Hemoglobin a1c and self-monitored average glucose: validation of the dynamical tracking ea1c algorithm in type 1 diabetes. *J Diabetes Sci Technol* (2016) 10:330–5. doi: 10.1177/1932296815608870

13. Beck RW, Connor CG, Mullen DM, Wesley DM, Bergenstal RM. The fallacy of average: how using hba1c alone to assess glycemic control can be misleading. *Diabetes Care* (2017) 40:994–9. doi: 10.2337/dc17-0636

14. Fan W, Zheng H, Wei N, Nathan DM. Estimating hba1c from timed self-monitored blood glucose values. *Diabetes Res Clin Pract* (2018) 141:56–61. doi: 10.1016/j.diabres.2018.04.023

15. Bergenstal RM, Beck RW, Close KL, Grunberger G, Sacks DB, Kowalski A, et al. Glucose management indicator (gmi): a new term for estimating a1c from continuous glucose monitoring. *Diabetes Care* (2018) 41:2275–80. doi: 10.2337/dc18-1581

16. Leelarathna L, Beck RW, Bergenstal RM, Thabit H, Hovorka R. Glucose management indicator (gmi): insights and validation using guardian 3 and navigator 2 sensor data. *Diabetes Care* (2019) 42:e60–1. doi: 10.2337/dc18-2479

17. Perlman JE, Gooley TA, McNulty B, Meyers J, Hirsch IB. Hba1c and glucose management indicator discordance: a real-world analysis. *Diabetes Technol Ther* (2021) 23:253–8. doi: 10.1089/dia.2020.0501

18. Shah VN, Vigers T, Pyle L, Calhoun P, Bergenstal RM. Discordance between glucose management indicator and glycated hemoglobin in people without diabetes. *Diabetes Technol Ther* (2023) 25:324–8. doi: 10.1089/dia.2022.0544

19. Oriot P, Hermans MP. "mind the gap please": estimated vs. measured a1c from continuous measurement of interstitial glucose over a 3-month period in patients with type 1 diabetes. *Acta Clinica Belgica* (2020) 75:109–15. doi: 10.1080/17843286.2018.1561780

20. Hu Y, Shen Y, Yan R, Li F, Ding B, Wang H, et al. Relationship between estimated glycosylated hemoglobin using flash glucose monitoring and actual measured glycosylated hemoglobin in a chinese population. *Diabetes Ther* (2020) 11:2019–27. doi: 10.1007/s13300-020-00879-x

21. Xu Y, Dunn TC, Ajjan RA. A kinetic model for glucose levels and hemoglobin a1c provides a novel tool for individualized diabetes management. *J Diabetes Sci Technol* (2021) 15:294–302. doi: 10.1177/1932296819897613

22. Xu Y, Bergenstal RM, Dunn TC, Ajjan RA. Addressing shortfalls of laboratory hba1c using a model that incorporates red cell lifespan. *Elife* (2021) 10:e69456. doi: 10.7554/eLife.69456

23. Harris CR, Millman KJ, van der Walt SJ, Gommers R, Virtanen P, Cournapeau D, et al. Array programming with numPy. *Nature* (2020) 585:357–62. doi: 10.1038/s41586-020-2649-2

24. Virtanen P, Gommers R, Oliphant TE, Haberland M, Reddy T, Cournapeau D, et al. SciPy 1.0: fundamental algorithms for scientific computing in python. *Nat Methods* (2020) 17:261–72. doi: 10.1038/s41592-019-0686-2

25. Pedregosa F, Varoquaux G, Gramfort A, Michel V, Thirion B, Grisel O, et al. Scikit-learn: machine learning in python. *J Mach Learn Res* (2011) 12:2825–30. doi: 10.48550/arXiv.1201.0490

26. Bailey R, Calhoun P, Bergenstal RM, Beck RW. Assessment of the glucose management indicator using different sampling durations. *Diabetes Technol Ther* (2023) 25:148–50. doi: 10.1089/dia.2022.0284

Abstract #133765

ISPOR
Improving healthcare decisions

Multistakeholder Healthcare Cooperative: A New Paradigm for Healthcare Delivery

Javadekar N[1], Javadekar AN[2]
[1]MMRS-Maharashtra Medical Research Society,MMFHA Joshi hospital Pune, Erandawane, Pune, India,
[2]D.Y.Patil Medical College, Pimpri, Pune, Maharashtra, India

OBJECTIVES: To analyse healthcare system with financial engineering perspective to optimise the solution .

The healthcare delivery system in India is facing challenges to meet sustainable development goals by 2030. Government has a shortage of funds and 60% of the population pays from pocket for health care. This pushes many on the borders below the poverty line due to catastrophic out-of-pocket health expenditures.Healthcare demand and costs are rising due to the aging population and newer health technologies. Increased Expectations from medical treatment lead to frustration when the treatment fails to deliver desired outcomes, which leads to cases of violence against the medical community.

METHODS: The healthcare delivery system was analyzed using a **Financial engineering perspective** with the objective of optimising the outcomes . Three major areas of financial engineering that are most relevant to the risk analysis/management needs of health care organizations are stochastic analysis and value at risk,portfolio optimisation and asset liability management,and distributed decision making and agency theory.Governments desire to maximize the health of the citizens at minimum costs, and people desire good health. Healthcare providers such as doctors and hospitals are assumed to be working towards maximizing consumption. Diagnostic centers and the pharma industry are purely profit-oriented.

RESULTS: The multistakeholder system is a complex system and requires the meaningful cooperation of all the players to optimize the outcomes. Stakeholder management(**STM**) lies at the heart of **FIR**(fourth industrial revolution).Thus cooperative society may be a better model for delivery of health care in a complex multistakeholder environment with uncertain outcomes.

CONCLUSIONS: Co-operatives in healthcare may offer solutions to the shortage of funds,lack of access, and also help deliver inclusive and patient-centered care. India has had a rich experience in the cooperative sector and there is a scope for introducing healthcare cooperatives as a novel model of healthcare delivery, to achieve universal health coverage by 2030.

Abstract ID#:
133765
Submitter's E-mail Address:
narendrajavadekar@gmail.com

Program Selection:
Research

Preferred Presentation Format:
Either poster or podium

Research Study Approach:
Conceptual Papers

Main Topic/Taxonomy:
Organizational Practices

Subtopics:
Does Not Apply: Does Not Apply

Primary Specific Diseases & Cond./Specialized Treatment Areas:
No Additional Disease & Conditions/Specialized Treatment Areas

Additional Diseases & Conditions/Specialized Treatment Areas:
No Additional Disease & Conditions/Specialized Treatment Areas

Guarantor:
Narendra S.Javadekar

Session Assignment:
Organizational Practices

First author

Presenting Author

Narendra Javadekar, M.D (MED), DNB(MED),M.A(ECONOMICS)
Research Department
MMRS-Maharashtra Medical Research Society,MMFHA Joshi hospital Pune
778, Shivajinagar
Opposite Kamla Nehru Park
Erandawane, Pune, 411004
India
Phone Number: 9822091218
Email Address: narendrajavadekar@gmail.com
* Membership Number 3101011

Second author

Archana Narendra Javadekar, M.D.D.N.B.(Psychiatry)
Psychiatry
D.Y.Patil Medical College, Pimpri
45 Sahawas society
Karvenagar
Pune, Maharashtra, 411052
India
Phone Number: 9822041271
Email Address: archanajavadekar@gmail.com

Submitter

Archana Narendra Javadekar, M.D.D.N.B.(Psychiatry)
Psychiatry
D.Y.Patil Medical College, Pimpri
45 Sahawas society

Organizational Practices

OP1
STROKE TREATMENT UNITS: REQUIREMENTS AND RECOMMENDATIONS

Slavchev G,[1] Dacheva A,[2] Djambazov S,[3] Vutova Y[4]
[1]Medtronic International Trading Sàrl, Istanbul, 34, Turkey, [2]Medtronic International Trading Sàrl, Tolochenaz, Switzerland, [3]Medical University Pleven, Sofia, 23, Bulgaria, [4]HTA Ltd., Sofia, 22, Bulgaria

Objectives: This study aimed to outline the requirements and recommendations for establishing specialized stroke treatment units. ***Methods:*** The criteria for specialized stroke treatment units were categorized into seven areas and analyzed based on existing recommendations and guidelines. These areas included infrastructure, early diagnosis, diagnostic and therapeutic infrastructure, therapeutic interventions, multidisciplinary mobilization and rehabilitation, expertise of medical staff, and emergency departments. ***Results:*** The infrastructure of a specialized stroke treatment unit should consist of two functional segments: Segment A for acute phase treatment and monitoring, and Segment B for post-acute phase treatment. Rapid neurological assessment and access to a neurologist or internist trained in stroke treatment are crucial within 30 minutes of admission. Diagnostic procedures such as CT scans, echocardiography, and Doppler or duplex sonography should be available within specific timeframes. Therapeutic interventions, including thrombolysis and thrombectomy, should be initiated promptly. Multidisciplinary mobilization and rehabilitation should be provided, addressing nursing care, physiotherapy, speech therapy, cognitive rehabilitation, and patient education. The expertise of physicians and nursing staff should be continuously developed through training programs. ***Conclusions:*** The establishment of specialized stroke treatment units requires adherence to specific requirements and recommendations. These units should have appropriate infrastructure, rapid and accurate diagnostic procedures, efficient therapeutic interventions, and multidisciplinary mobilization and rehabilitation. Ongoing training of medical staff is essential to maintain expertise. Access to emergency departments with trained professionals is crucial for continuous stroke care. Implementing these recommendations can improve stroke treatment outcomes and enhance patient recovery.

OP3
SINGLE-USE VS REUSABLE ENDOSCOPY REPROCESSING: AN EFFICIENCY SURVEY OF NURSES AND TECHNICIANS

Hoffman D, Haislip I, **Dehlholm-Lambertsen E,** Cool C
Ambu USA, Columbia, MD, USA

Objectives: Numerous studies have highlighted the potential time savings single-use endoscopes (SUEs) may afford facilities when compared to reusable endoscopes (REs) due to their ability to eliminate post-procedure cleaning. This time savings may not only allow for more procedures to be performed, but free up the resources and time of individuals responsible for cleaning both the procedure rooms and REs. The purpose of this survey was to evaluate the impact SUEs could have on the individuals responsible for procedure room turnover and RE reprocessing. ***Methods:*** Clinical training specialists across the United States distributed surveys to nurses, reprocessing technicians, and others involved in endoscope reprocessing. Data collection took place from September 2022 to February 2023. Proportions were calculated using each question's applicable respondents. ***Results:*** 52 participants participated in the survey. 100% believed using SUEs instead of REs could save time and allow them to spend more time on imperative tasks, with 66% saving 4+ hrs/week and 17% saving 15+ hrs/week. When considering time savings, 70% believed they would be able to reallocate 4+ hrs/week and 13% believed they could reallocate 15+ hrs/week. Additionally, 11% of individuals felt that SUEs could reduce 6+ hrs/week of after-hours and/or weekend time. Finally, 89% of reprocessing technicians felt that eliminating the reprocessing of just one type of scope would reduce the pressure to keep up with the demands of cleaning/reprocessing other types of scopes and equipment. ***Conclusions:*** SUEs may not only save employees time by eliminating endoscope reprocessing but allow them to spend time doing more imperative tasks and reduce job pressures. All respondents felt that utilizing only SUEs could save time and over 17% felt they could save 15+ hrs/week. If widely adopted, facilities may not only see a reduction in costs, but an increase in time savings, employee morale, and elimination of reprocessing related risks.

OP4
SCIENTIFIC COMMUNICATION PLANS IN HEALTH ECONOMICS AND REAL-WORLD EVIDENCE

Belli K, Bernz I, Pereira RG, Ribeiro A, Gennaro C
IQVIA Solutions, São Paulo, SP, Brazil

Objectives: To review and report reasons to include a scientific communication plans (SCP) in projects of health economics and real-world evidence globally. ***Methods:*** We conducted a narrative literature review to map reasons presented in literature for support implementations of SCP for research projects. We discussed the main reasons founded to support future adoptions of SCP in health economics and outcomes research. ***Results:*** The use of SCP is an outline to guide effective communication for various audiences. Some projects are including a roadmap with milestones for sharing their methodologies, results and future steps for different audiences like other scientists, patients, policymakers, funding agencies. The main reasons to encourage an organization of scientific communication plans covered in this review were: collaboration, resource allocation, transparency, reproducibility and dissemination. A SCP allows researchers around the world to identify potential synergies and collaborate effectively in real-world studies, for example. It also permits institutions, stakeholders, policymakers and funding agencies to save and allocate resources more strategically. A SCP allows the scientific community to evaluate details from each study increasing the transparency and reproducibility. A structured SCP can contribute to dissemination of science, contributing to collective understanding of science. It also facilitates future research and inspires new ideas. ***Conclusions:*** The use of SCP has a main objective to expand the reach of science across different areas around the globe, as in health economics and real-world evidence. Including a strategy for SCP inside projects can promote collaboration and improve resource allocation. Also allows transparency, reproducibility and dissemination of science in different areas.

OP5
MULTISTAKEHOLDER HEALTHCARE COOPERATIVE: A NEW PARADIGM FOR HEALTHCARE DELIVERY

Javadekar N
MMRS-Maharashtra Medical Research Society,MMFHA Joshi hospital Pune, Pune, MH, India

Objectives: To analyse healthcare system with financial engineering perspective to optimise the solution . The healthcare delivery system in India is facing challenges to meet sustainable development goals by 2030. Government has a shortage of funds and 60% of the population pays from pocket for health care. This pushes many on the borders below the poverty line due to catastrophic out-of-pocket health expenditures.Healthcare demand and costs are rising due to the aging population and newer health technologies. Increased Expectations from medical treatment lead to frustration when the treatment fails to deliver desired outcomes, which leads to cases of violence against the medical community. ***Methods:*** The healthcare delivery system was analyzed using a **Financial engineering perspective** with the objective of optimising the outcomes . Three major areas of financial engineering that are most relevant to the risk analysis/management needs of health care organizations are stochastic analysis and value at risk,portfolio optimisation and asset liability management,and distributed decision making and agency theory.Governments desire to maximize the health of the citizens at minimum costs, and people desire good health. Healthcare providers such as doctors and hospitals are assumed to be working towards maximizing consumption. Diagnostic centers and the pharma industry are purely profit-oriented. ***Results:*** The multistakeholder system is a complex system and requires the meaningful cooperation of all the players to optimize the outcomes. Stakeholder management(**STM**) lies at the heart of **FIR** (fourth industrial revolution).Thus cooperative society may be a better model for delivery of health care in a complex multistakeholder environment with uncertain outcomes. ***Conclusions:*** Co-operatives in healthcare may offer solutions to the shortage of funds,lack of access, and also help deliver inclusive and patient-centered care. India has had a rich experience in the cooperative sector and there is a scope for introducing healthcare cooperatives as a novel model of healthcare delivery, to achieve universal health coverage by 2030.

OP6
OVERCROWDING AND BOARDING TIME: EMERGENCY DEPARTMENT PERFORMANCE AND IMPACTING FACTORS

Foglia E,[1] Asperti F,[1] **Bellavia D,**[1] Schettini F,[1] Bellini R,[2] Boverio R,[2] Gualco C,[1] Zanelli C,[1] Porazzi E[1]
[1]LIUC University, Castellanza, VA, Italy, [2]Azienda Ospedaliera SS. Antonio e Biagio e Cesare Arrigo, Alessandria, Italy, Italy

Objectives: Higher boarding times (BTs) usually affect the Emergency Departments' (EDs) activities, resulting in a lower care quality level for patients, waiting for an inpatient bed. This study aims to evaluate the different EDs performance indicators affecting BT. ***Methods:*** Real-life data were collected in an ED in Northern Italy, considering the years 2019-2022, and referring to 189,976 accesses (134,199 adults and 55,777 pediatrics). The following KPIs were assessed: time between ED access and the first visit, BT, ED overall stay, ED repeated access within 72 hours. Both the National Emergency Department Overcrowding Scale (NEDOCS) and the Emergency Department Working Index (EDWIN) were adopted. All measures were compared to the national standards. A bivariate correlation was performed to explain endogenous and exogenous factors, that could impact on the patients' BT. ***Results:*** Time between ED access and the first visit results over the national standards, for all the patients, except for white and green patients (referring to pediatric department). Repeated accesses within 72 hours increased for white and green patients; a decreasing trend was registered for red and yellow patients, especially in the children's pediatric department. Stratifying the accesses and evaluating the NEDOCS index, in the pediatric department overcrowding situations were demonstrated only for the light-blue and green patients. The bivariate analyses revealed that time band (β=-0.057; p-value=0.000), patient's code (β=-0.028; p-value=0.005), and ED organizational assets (β=0.039; p-value=0.000) could affect the BT, with an increase during the night and for the less complex codes. ***Conclusions:*** BT resulted higher at night, as a consequence of the reduced number of recovered patients, increasing the overcrowding. The overall process time is enlarged over the years 2020-2021, also due to the COVID-19 spread; better results emerged in 2022. EDWIN and NEDOCS indexes could be considered as relevant indicators, providing more comprehensive information for understanding EDs dynamics and improving EDs management.